

See discussions, stats, and author profiles for this publication at: <https://www.researchgate.net/publication/273778142>

# Novel Multitarget-Directed Ligands (MTDLs) with Acetylcholinesterase (AChE) Inhibitory and Serotonergic Subtype 4 Receptor (5-HT<sub>4</sub>R) Agonist Activities As Potential Agents against...

ARTICLE *in* JOURNAL OF MEDICINAL CHEMISTRY · MARCH 2015

Impact Factor: 5.45 · DOI: 10.1021/acs.jmedchem.5b00115 · Source: PubMed

---

CITATIONS

2

READS

156

---

## 20 AUTHORS, INCLUDING:



[Patrizia Giannoni](#)

Institut de Génomique Fonctionnelle,

20 PUBLICATIONS 215 CITATIONS

[SEE PROFILE](#)



[Samir Yahiaoui](#)

University Joseph Fourier - Grenoble 1

18 PUBLICATIONS 225 CITATIONS

[SEE PROFILE](#)



[Thomas Freret](#)

Université de Caen Normandie

60 PUBLICATIONS 949 CITATIONS

[SEE PROFILE](#)



[Jana Sopkova-de Oliveira Santos](#)

Université de Caen Normandie

128 PUBLICATIONS 1,618 CITATIONS

[SEE PROFILE](#)

# Novel Multitarget-Directed Ligands (MTDLs) with Acetylcholinesterase (AChE) Inhibitory and Serotonergic Subtype 4 Receptor (5-HT<sub>4</sub>R) Agonist Activities As Potential Agents against Alzheimer's Disease: The Design of Donecopride

Christophe Rochais,<sup>\*,†</sup> Cédric Lecoutey,<sup>†</sup> Florence Gaven,<sup>‡,§,||</sup> Patrizia Giannoni,<sup>‡,§,||</sup> Katia Hamidouche,<sup>⊥</sup> Damien Hedou,<sup>†</sup> Emmanuelle Dubost,<sup>†</sup> David Genest,<sup>†</sup> Samir Yahiaoui,<sup>†</sup> Thomas Freret,<sup>⊥</sup> Valentine Bouet,<sup>⊥</sup> François Dauphin,<sup>⊥</sup> Jana Sopkova de Oliveira Santos,<sup>†</sup> Céline Ballandonne,<sup>†</sup> Sophie Corvaisier,<sup>†,⊥</sup> Aurélie Malzert-Fréon,<sup>†</sup> Remi Legay,<sup>†</sup> Michel Boulouard,<sup>⊥</sup> Sylvie Claeysen,<sup>‡,§,||</sup> and Patrick Dallemande<sup>\*,†</sup>

<sup>†</sup>UNICAEN, CERMN (Centre d'Etudes et de Recherche sur le Médicament de Normandie), F-14032 Caen, France

<sup>‡</sup>CNRS, UMR-5203, Institut de Génomique Fonctionnelle, F-34000 Montpellier, France

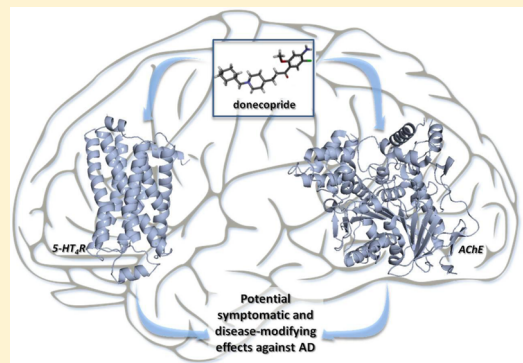
<sup>§</sup>Inserm, U1191, F-34000 Montpellier, France

<sup>||</sup>Université de Montpellier, UMR-5203, F-34000 Montpellier, France

<sup>⊥</sup>UNICAEN, GMPC5 (Groupe Mémoire et Plasticité comportementale), F-14032 Caen, France

## Supporting Information

**ABSTRACT:** In this work, we describe the synthesis and in vitro evaluation of a novel series of multitarget-directed ligands (MTDL) displaying both nanomolar dual-binding site (DBS) acetylcholinesterase inhibitory effects and partial 5-HT<sub>4</sub>R agonist activity, among which donecopride was selected for further in vivo evaluations in mice. The latter displayed procognitive and antiamnesic effects and enhanced sAPP $\alpha$  release, accounting for a potential symptomatic and disease-modifying therapeutic benefit in the treatment of Alzheimer's disease.



## INTRODUCTION

Alzheimer's disease (AD), the most common form of dementia among the elderly, is a chronic, progressive and degenerative disorder of the brain featuring impairments in cognitive functions, especially memory processes.<sup>1</sup> As of 2013, there were an estimated 44.4 million people with dementia worldwide.<sup>2</sup> By 2050, it is projected that this figure will have increased to over 115 million. Not only are there numerous reasons for concern, but AD and dementia have an enormous impact on societies.<sup>3</sup> The total estimated worldwide costs of dementia were U.S. \$604 billion in 2010. Given that the pathogenesis of AD is complex and related to the abnormality and dysfunction of multisystems, the prevention and treatment of AD have remained elusive to date. Most of the current treatments produce only symptomatic benefits through the catalytic inhibition of acetylcholinesterase (AChE).<sup>4</sup> So far, investigational new drugs that have reached clinical trials have been targeting amyloid aggregation or neurofibrillary tangle production linked to the abnormality of protein  $\tau$  phosphor-

ylation. Nevertheless, many of these trials recently failed, and some of these failures have been attributed to the extreme selectivity of the tested drugs against a single target, disregarding the fact that neurodegenerative syndromes involve multiple pathogenic factors.<sup>5,6</sup> Consequently, efficient treatments should associate several drugs whose actions are oriented toward several targets involved in the pathogenesis. These drugs could be combined in a cocktail (multiple-medication therapy) or in a single formulation (multiple-compounded medication). However, these approaches might be disadvantageous for patients with respect to compliance difficulties, drug-drug interactions, problems of bioavailability, and metabolism.

These issues are difficult to solve when the drugs present different pharmacokinetic profiles.<sup>7,8</sup> Today, a new concept is emerging; also called "hybride molecules", "designed multiple ligands", or "multitarget-directed ligands" (MTDLs), it

Received: January 21, 2015

describes those compounds that are effective in treating complex diseases because of their ability to interact with the multiple targets thought to be responsible for the disease pathogenesis.<sup>9–22</sup> Besides reducing the pharmacokinetic and interaction problems linked to multiple-medication therapy, MTDLs generally show a synergistic effect. They could be particularly useful in the treatment of neurodegenerative diseases like AD.<sup>23–34</sup> Recently, hybrid agents with a dual mode of action against AD have been described. One of the most widely adopted approaches in the field has been to modify the molecular structure of an AChE inhibitor (AChEI) in order to complement it with additional biological activities that are useful for treating AD, like M2 receptor antagonism,<sup>35</sup> direct inhibition of amyloid beta peptide ( $A\beta$ ) aggregation,<sup>36–41</sup> AChE-dependent amyloid aggregation inhibition (dual-binding site [DBS] inhibitors),<sup>42–46</sup> or providing it with antioxidant properties<sup>47–50</sup> linked to MAO-B inhibition,<sup>51–54</sup> calcium channel blockage,<sup>55,56</sup> or control oxidative damage properties.<sup>57</sup> Within this scope, we very recently described the design of **1** (donecopperide), a novel drug candidate exhibiting, for the first time, both in vitro DBS AChE inhibitory activity and a serotonergic subtype 4 receptor ( $5-HT_4R$ ) partial agonist effect, promoting the secretion of the neurotrophic protein sAPP $\alpha$  in an in vitro cellular model and finally leading to an in vivo procognitive effect in mice.<sup>58</sup> Donecopperide was conceived as a structural compromise between donepezil (DPZ), an AChEI drug, and **2** (RS67333),<sup>59</sup> a  $5-HT_4R$  agonist (Figure 1).

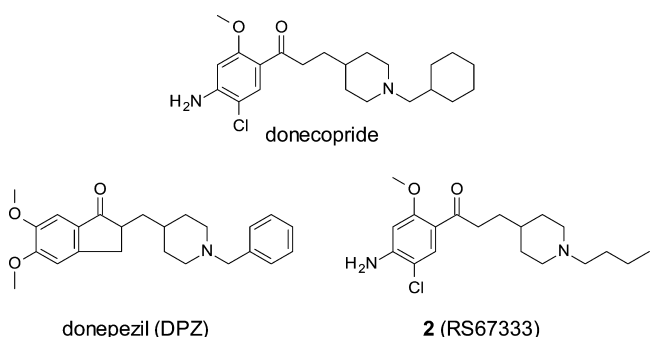


**Figure 1.** Structure of donecopperide, DPZ, and **2**.

This MTDL profile seems to confer to donecopperide the ability to display both improvements in cholinergic neurotransmission (through the catalytic inhibition of AChE and the  $5-HT_4R$ -dependent release of ACh) and in the inhibition of  $A\beta$  accumulation and aggregation. This second effect would be possible through the nonamyloidogenic  $5-HT_4R$ -dependent cleavage of the precursor of  $A\beta$  and the consequent promotion of the neurotrophic protein, sAPP $\alpha$ , as well as through the interaction of donecopperide with the peripheral anionic site (PAS) of AChE, which is able to counteract the chaperone role played by the latter in  $A\beta$  aggregation. Finally, these complementary activities could exert both symptomatic and disease-modifying effects for AD treatment (Figure 2).<sup>60</sup>

The present article aims to describe the discovery of donecopperide in the context of the chemical series from which it was selected in order to establish some structure–activity relationships (SARs) as well as to describe additional in vivo experiments useful for precisely determining its pharmacological profile.

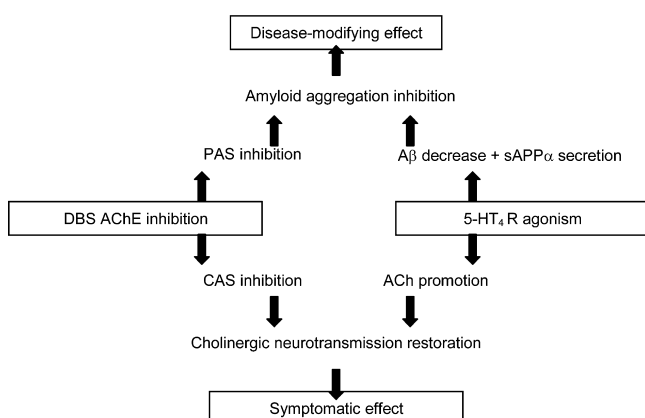


**Figure 2.** Pleiotropic interest of DBS AChEI/5-HT<sub>4</sub>R agonists.

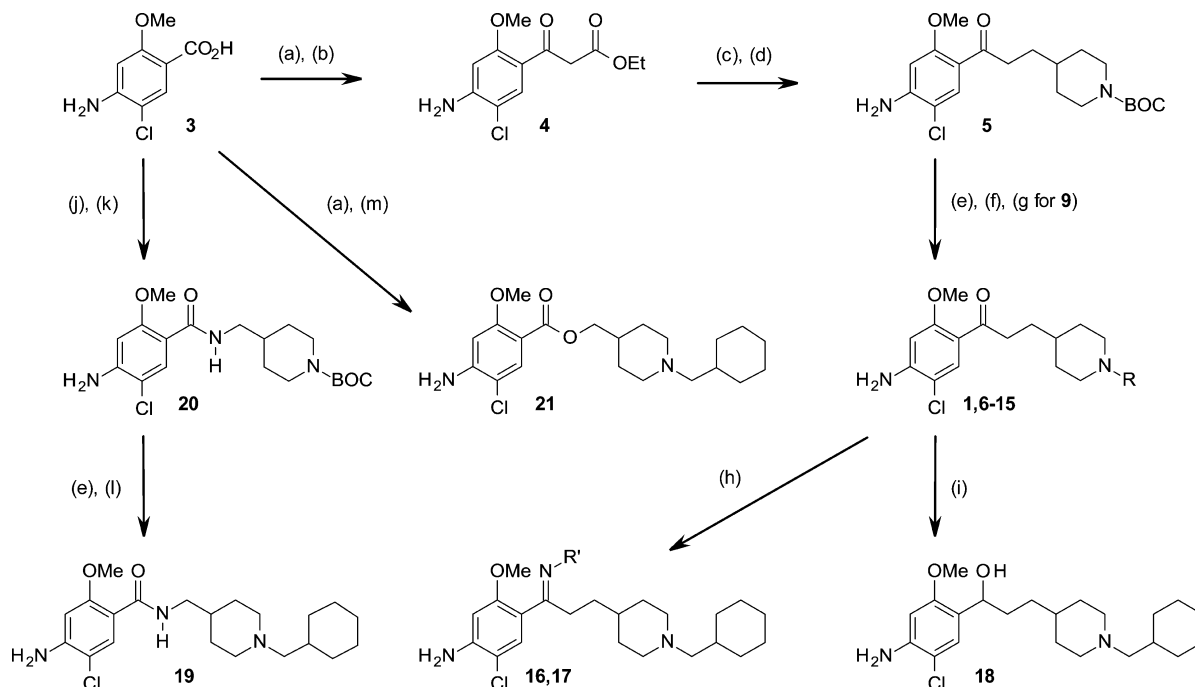
## RESULTS

**Chemistry.** Donecopperide was obtained according to a previously reported multistep sequence<sup>58</sup> starting from 4-amino-5-chloro-2-methoxybenzoic acid (**3**) (Scheme 1). The sequence starts with the synthesis of a  $\beta$ -ketoester (**4**) with a 62% yield, which took place after the carbonyldiimidazole (CDI) activation of the carboxylic acid group of **3**. The methylpiperidine moiety was then installed through a nucleophilic substitution using N-Boc 4-(iodomethyl)-piperidine carboxylate at room temperature to avoid the risk of a double substitution, immediately followed by a saponification–decarboxylation sequence with hydroalcoholic potassium hydroxide which gave **5** in an 86% yield. **1** was finally obtained in 44% yield through the TFA-N-deprotection of **5**, immediately followed by another nucleophilic substitution with bromomethylcyclohexane. Starting from **5** and using various alkyl- and arylmethyl bromides according to these experimental conditions, numerous other N-substituted derivatives (**6–15**) were obtained. Finally, the oxime (**16**) and methyloxime (**17**) of donecopperide were selectively obtained in excellent yield under their *E* form (according to their X-ray structure) under treatment using hydroxylamine and methoxylamine, respectively. The reduction of its carbonyl group, using sodium borohydride, afforded the hydroxyl derivative (**18**) in an 62% yield.

The anisamide **19**, an analog of donecopperide, was issued from a peptidic coupling between **3** and N-Boc aminomethylpiperidine and affording **20** which was then N-deprotected and substituted with a methylcyclohexyl group under treatment with bromomethylcyclohexane. Finally the ester **21** was synthesized in 31% yield through the esterification of **3** using the commercially available N-methylcyclohexyl-4-hydroxymethylpiperidine.

**In Vitro Results.** All the synthesized compounds were evaluated as potential inhibitors of human AChE and equine BuChE as well as potential ligands for guinea pig  $5-HT_4R$  (Table 1). In these tests, DPZ was used as an AChEI control and **2** as both a  $5-HT_4R$  ligand and an AChEI control since we recently reported its MTDL pharmacological profile.<sup>58</sup>

The results of these in vitro evaluations are reported in a double-entry table where we also reported the results concerning **2** and DPZ (Table 2). Among the 16 tested compounds, two of them (compounds **17**, **18**) were found to be almost inactive against the two designed targets. One of them (compound **16**) is highly inhibitor of AChE, but it is almost devoid of affinity for  $5-HT_4R$ , as is the case for DPZ.

Scheme 1. Synthetic pathways for access to compounds 1 and 6–21<sup>a</sup>

<sup>a</sup>Conditions and reagents: (a) CDI, THF; (b) KO<sub>2</sub>CCH<sub>2</sub>CO<sub>2</sub>Eti, MgCl<sub>2</sub>, THF; (c) N-Boc 4-iodomethylpiperidine, K<sub>2</sub>CO<sub>3</sub>, DMF; (d) KOH, EtOH/H<sub>2</sub>O; (e) TFA, DCM; (f) RBr, K<sub>2</sub>CO<sub>3</sub>, DMF; (g) HCl/EtOH; (h) H<sub>2</sub>NOR', HCl, pyridine; (i) NaBH<sub>4</sub>, MeOH; (j) TEA, DMF; (k) HOBT, EDCI-HCl, N-Boc 4-aminomethylpiperidine, DMF; (l) CyHexCH<sub>2</sub>Br, K<sub>2</sub>CO<sub>3</sub>, DMF; (m) N-CyHexCH<sub>2</sub>-4-hydroxymethylpiperidine, NaH, THF.

Conversely, four compounds (**6**, **7**, **19**, **21**) appear to be good ligands for 5-HT<sub>4</sub>R, but they do not show any AChE inhibitory effects. Finally, nine compounds (**1**, **8–10**, **11–15**) could be considered as MTDL since they exhibit both a  $K_{i(5\text{-HT}_4\text{R})} \leq 20$  nM and an  $IC_{50(\text{AChE})} \leq 400$  nM, as was found with **2**. These compounds further showed a good selectivity toward AChE versus BuChE.

The most potent compounds (**1**, **8–10**, **13**) were further evaluated to establish their affinity and their pharmacological profile with regard to their potential agonist effects toward human 5-HT<sub>4</sub>R and their capacity to bind to the PAS of electric eel AChE using the propidium iodide displacement test (Table 3).

By virtue of its in vitro activities and selectivity toward AChE and 5-HT<sub>4</sub>R as well as its good druggability parameters (water solubility, blood-brain barrier [BBB] cross-membrane penetration, P-gp inhibition, mutagenicity, cytotoxicity, hERG affinity and so on),<sup>58</sup> compound **1** was selected for in silico and in vivo studies aiming to evaluate its potential in AD treatment. We named it donecopride.

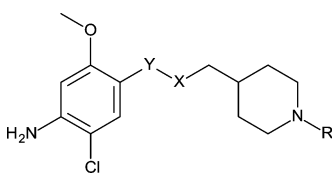
**In Silico Results.** Ahead of the in silico study of donecopride, its three-dimensional structure was identified via the X-ray diffraction technique. The analysis carried out on the donecopride crystal showed that two molecules are present in the asymmetric unit, which differs principally in the position of the cyclohexane ring. As the crystal space group is a centrosymmetric one, another conformer, related to the asymmetric unit by a symmetric center, is present in the crystal for both molecules of the asymmetric unit (Figure 3). Interestingly, the carbonyl group and the methoxy substituent of the benzene ring point in opposite directions in all solved structures. The four conformers observed in the crystal were used for the docking studies, and the opposite mutual

orientation of the carbonyl and methoxy groups was used as a criterion for the selection of docking poses.

Docking studies of donecopride were then performed in a human AChE structure (PDB ED: 4EY7)<sup>62</sup> as well as in a human 5-HT<sub>4</sub>R model, as previously reported by us.<sup>63</sup>

First, the four conformers of donecopride from the crystal structure (protonated on the piperidine ring) were docked separately into the (*h*)5-HT<sub>4</sub>R homology model that was built using the  $\beta_2$ -adrenergic receptor crystal structure as a template (PDB ED: 2RH1).<sup>63,64</sup> In the selected pose (Figure 4A, mean ChemPLP fit = 78.61), the basic piperidine nitrogen interacts with Asp<sub>100</sub> (consistent with the constraint used during docking), and an additional polar interaction could be engaged through this basic nitrogen and the Tyr<sub>302</sub> hydroxyl group. The benzene ring is oriented toward the transmembrane helix 5 (TMS) (in yellow in Figure 4A), and the amino substituent on the benzene ring forms a hydrogen bond with the Ser<sub>197</sub> hydroxyl group. In this position the benzene ring is surrounded by several aromatic residues, oriented perpendicularly to it.

During the docking of donecopride conformers into (*h*)AChE, a water molecule interacting with the protonated piperidine ring of DPZ was conserved (residue number 931). In the selected scoring pose (Figure 4B, mean ChemPLP Score = 109.59), the donecopride orientation was closed to DPZ and reproduced its interactions: (1) the charged nitrogen of the piperidine ring was oriented in a position that was suitable for interaction with the water molecule in the proximity of Tyr<sub>337</sub> and Tyr<sub>341</sub>; (2) the donecopride carbonyl formed a hydrogen bond with NH of the Phe<sub>295</sub> backbone; (3) the benzene ring was positioned in a parallel manner to the Trp<sub>286</sub> indole ring of the PAS at a 3.5 Å distance to favor a  $\pi$ -stacking interaction (which is in accordance with the result of the propidium displacement test results); and (4) the cyclohexane ring

**Table 1.** (*h*)AChE Inhibitory Activity and Selectivity versus (*eq*)BuChE and (*gp*)5-HT<sub>4</sub>R Affinity for DPZ, **2**, and compounds **1** and **6–21**


Compound	Y	X	R	( <i>h</i> )AChE IC <sub>50</sub> (nM) or % inhibition at 10 <sup>-5</sup> M	( <i>eq</i> )BuChE IC <sub>50</sub> (nM) or % inhibition at 10 <sup>-5</sup> M	( <i>gp</i> )5-HT <sub>4</sub> R Ki (nM)
DPZ	–	–	–	6 ± 0.6 n = 5 <sup>a</sup>	7,000 <sup>a</sup>	–
<b>1</b>	C=O	CH <sub>2</sub>		16 ± 5 n = 2 <sup>a</sup>	3,530 ± 50 n = 2 <sup>a</sup>	6.6 ± 3 n = 3
<b>2</b>	C=O	CH <sub>2</sub>	<i>n</i> Bu	403 ± 86 n = 2 <sup>a</sup>	–	9.3 ± 5 n = 3
<b>6</b>	C=O	CH <sub>2</sub>		937 ± 22 n = 2	6,600	14.8 ± 11 n = 3
<b>7</b>	C=O	CH <sub>2</sub>		577 ± 26 n = 2	47%	8.8 ± 4 n = 3
<b>8</b>	C=O	CH <sub>2</sub>		69 ± 6 n = 2	6,910	3.02 ± 0.2 n = 3
<b>9</b>	C=O	CH <sub>2</sub>		57 ± 3 n = 2	4,000	3.9 ± 5 n = 2
<b>10</b>	C=O	CH <sub>2</sub>		118 ± 7 n = 2	26%	2.50 ± 0.9 n = 3
<b>11</b>	C=O	CH <sub>2</sub>		222 ± 17 n = 2	6,340	8.2 ± 3 n = 3
<b>12</b>	C=O	CH <sub>2</sub>		321 ± 9 n = 2	4,340	4.9 ± 4 n = 3
<b>13</b>	C=O	CH <sub>2</sub>		8.5 ± 0.2 n = 2	1,835 ± 35 n = 2	14.3 ± 6 n = 3
<b>14</b>	C=O	CH <sub>2</sub>		45 ± 4 n = 2	9,165	20.4 ± 10 n = 3
<b>15</b>	C=O	CH <sub>2</sub>		121 ± 1 n = 2	46%	20.6 ± 11 n = 3
<b>16</b>	C=N-OCH <sub>3</sub>	CH <sub>2</sub>		24 ± 1 n = 2	7,080	193 ± 77 n = 3
<b>17</b>	C=N-OCH <sub>3</sub>	CH <sub>2</sub>		33%	7,420	105 ± 19 n = 3
<b>18</b>	CHOH	CH <sub>2</sub>		1,030 ± 57 n = 2	3,640	122 ± 71 n = 3
<b>19</b>	C=O	NH		45%	ND	2.25 ± 0.28 n = 3
<b>21</b>	C=O	O		2,720 ± 71 n = 2	4,100	0.95 ± 0.3 n = 3

<sup>a</sup>Results reported from Lecoutey et al.<sup>58</sup>

occupied the DPZ benzyl ring space (in the neighboring area of Trp<sub>86</sub>).

**In Vivo Results.** The data concerning the preliminary toxicological and pharmacological screening of donecopride (Table 4) showed no symptoms at subtoxic doses (around 7-fold less than the approximative LD<sub>50</sub>).

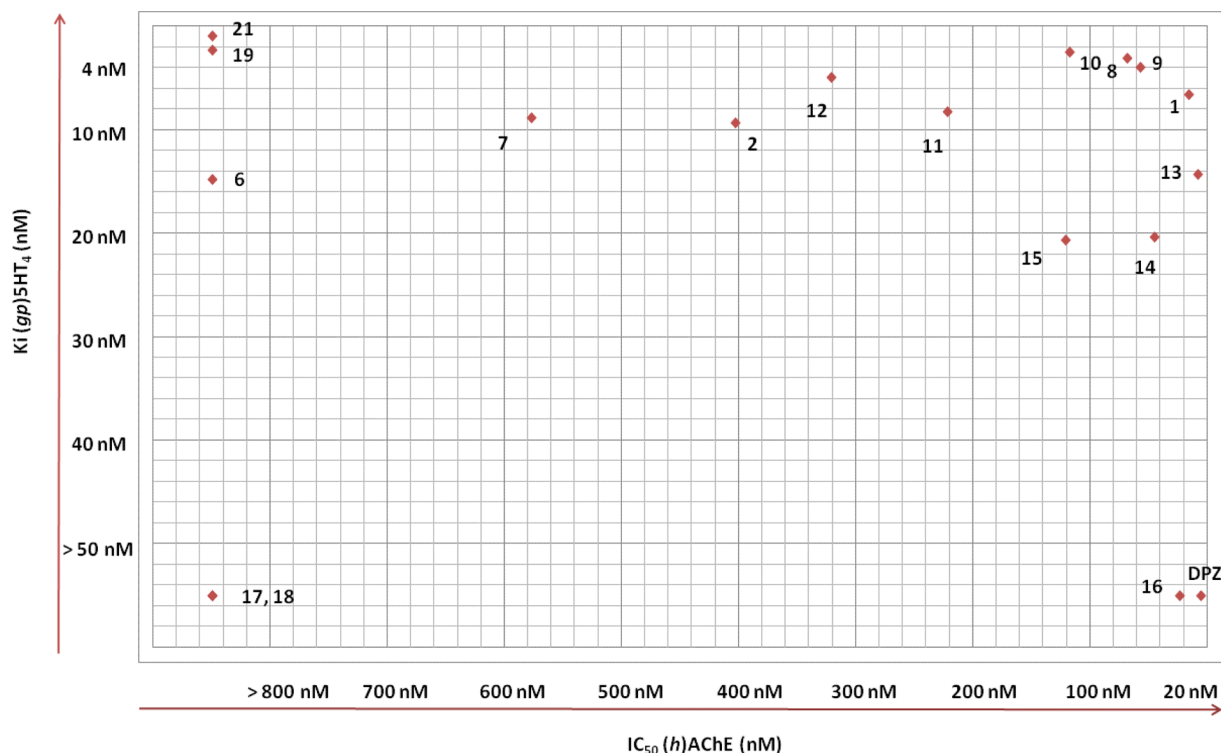
Thus, subsequent behavioral studies were realized at the maximum dose of 10 mg/kg. At the tested doses, donecopride demonstrated no effect on spontaneous locomotor activity (Figure 5).

We already showed that donecopride exhibited a procognitive effect with an improvement in memory performances, which was observed at 0.3 and 1 mg/kg on the object recognition test.<sup>58</sup> Moreover, in regards to scopolamine-

induced spontaneous alternation deficit, an antiamnesic effect was observed at doses starting from 0.3 mg/kg (Figure 6). Interestingly, a comparable effect has been obtained with the association of **2** to DPZ and with DPZ alone (1 mg/kg).

Finally, a decreased time of immobility was observed during the forced swimming test for the 0.3 mg/kg dose of donecopride, suggesting a slight antidepressant-like effect (Figure 7).

On the other hand, we have previously demonstrated that donecopride is able to increase sAPP $\alpha$  release in vitro in COS-7 cells transiently expressing 5-HT<sub>4</sub>R (EC<sub>50</sub> = 11.3 nM, E<sub>max</sub> = 22.5% of the maximum 5-HT response over the basal response).<sup>58</sup> In the present work, we administered one dose of donecopride (1 mg/kg) IP to C57BL/6 mice and collected

**Table 2.**  $^2\text{D}$  Representation of (*gp*)5-HT<sub>4</sub>R Affinity and (*h*)AChE Inhibitory Activity for Compounds 1, 6–21, DPZ, and 2**Table 3.** (*h*)5-HT<sub>4e</sub>R Binding Assay (Displacement of 1-(2-Methylsulfonylaminooethyl-4-piperidinyl)methyl-1-methyl-1*H*-indole-3-carboxylate (22) [ $^3\text{H}$ ]GR113808)<sup>61</sup>), (*h*)5-HT<sub>4e</sub>R Agonist Activity, And Propidium Iodide Competition Assay for Compounds 1, 8–10, 13

	(h)5-HT <sub>4e</sub> R			
	control ligand displacement			
	% inhibition at $10^{-6}$ M	% inhibition at $10^{-8}$ M	% control agonist response	propidium iodide displacement from ( <i>ee</i> ) AChE PAS % inhibition at $10^{-5}$ M
DPZ	—	—	—	$21.5 \pm 1.5$ <i>n</i> = 2 <sup>a</sup>
1	100	73	$48.3 \pm 0.9$ <i>n</i> = 3 <sup>a</sup>	$24 \pm 2$ <i>n</i> = 2 <sup>a</sup>
2	—	—	$48.7 \pm 5.2$ <i>n</i> = 3 <sup>a</sup>	—
8	100	58	48	20
9	99	46	58	20
10	100	69	20	30
13	100	41	65	13

<sup>a</sup>Results reported from Lecoutey et al.<sup>58</sup>

cerebrospinal fluid (CSF) 90 min after the injection. Quantification of sAPP $\alpha$  in the samples showed a slight increase in the neuroprotective APP fragment which is nonsignificant in these conditions (Figure 8). Further experiments taking into account the biodistribution of donecoperide are necessary to adjust the time point of CSF collection and to unequivocally conclude that donecoperide promotes *in vivo* sAPP $\alpha$  secretion.

## DISCUSSION

If we first try to establish some SAR from these results, we can point out that replacing the *n*-butyl group of 2 ( $K_{i[5\text{-HT}_4\text{R}]} = 9.33$

nM and  $IC_{50[\text{AChE}]} = 403$  nM) with a methyl-cyclopropyl group results in a dramatic decrease in AChE inhibition (see compound 6  $IC_{50[\text{AChE}]} = 937$  nM), while its 5-HT<sub>4</sub>R affinity is almost maintained ( $K_{i[5\text{-HT}_4\text{R}]} = 14.30$  nM). Substituting the piperidine moiety by a methylcyclobutyl group (compound 7) allows us to recover the 5-HT<sub>4</sub>R affinity of 2, but it does not totally restore its AChE inhibitory effect ( $IC_{50[\text{AChE}]} = 577$  nM). A larger methylcycloalkyl group, however, highly increases the activities of compounds 8, 1, and 9 toward the two targets ( $IC_{50[\text{AChE}]} < 100$  nM;  $K_{i[5\text{-HT}_4\text{R}]} < 10$  nM), thus rendering them as excellent MTDLs according to our criteria. The apparent degrees of freedom allowed for the nature of these alkyl groups are however quickly exceeded since replacing them by either an ethylcyclohexyl group (compound 11) or a methyl *ortho*-methylcyclohexyl group (compound 12) results in an important decrease in the AChE inhibitory activity, while the 5-HT<sub>4</sub>R affinity is maintained.

On the other hand, substituting the *n*-butyl group of 2 by a benzyl group, similar to those of DPZ, results in a dramatic increase in the AChE inhibition exerted by compound 13 ( $IC_{50[\text{AChE}]} = 8.5$  nM), while its 5-HT<sub>4</sub>R affinity is slightly decreased ( $K_{i[5\text{-HT}_4\text{R}]} = 14.30$  nM). This compound also appears to be as good an MTDL against the considered targets. Replacing its phenyl group by a *meta* (compound 14) or *para* (compound 15) pyridine group, however, leads to a decrease in 5-HT<sub>4</sub>R affinity ( $K_{i[5\text{-HT}_4\text{R}]} > 20$  nM) which appears to be particularly linked to the basic nature of the intracyclic nitrogen, since the methylpiperidine substituent in compound 9 dramatically restores it ( $K_{i[5\text{-HT}_4\text{R}]} = 2.50$  nM).

We can also point out the apparent importance of the carbonyl group in these structures for 5-HT<sub>4</sub>R affinity since compounds 16–18 do not bind to this target. However, the oxime 16 remains an excellent AChEI, almost as potent as DPZ. Conversely, the benzamide (19) and the benzoate (21) exhibit excellent 5-HT<sub>4</sub>R affinities in a low nanomolar range

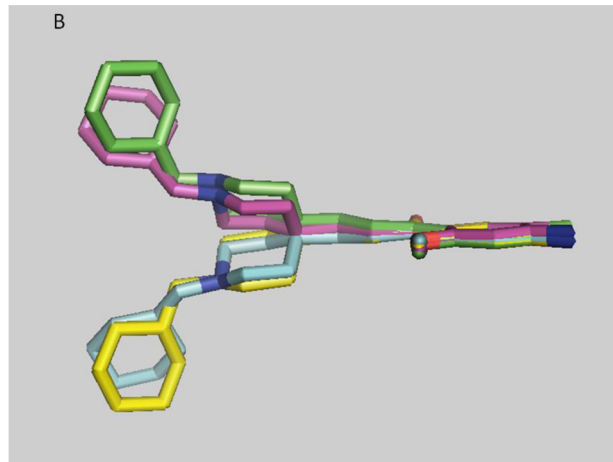
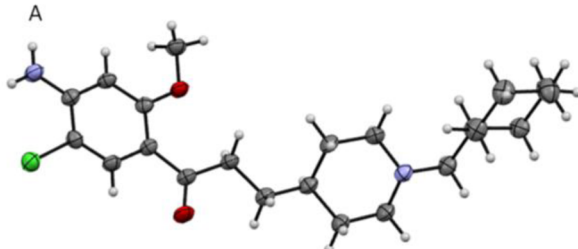


**Figure 3.** ORTEP diagram of donecopperide (A) and superposition of its four conformations in the crystal (B).

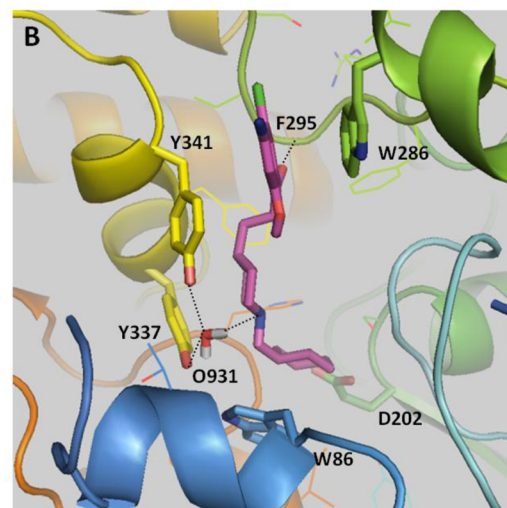
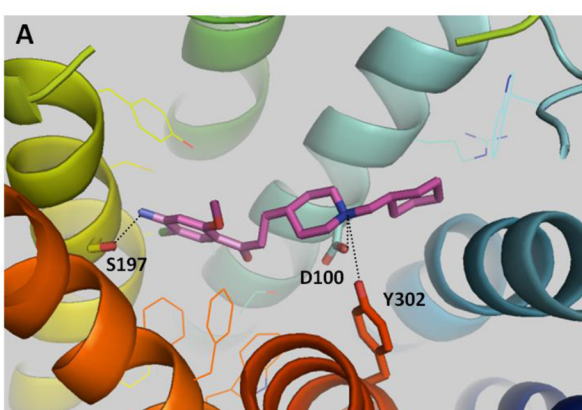


**Figure 4.** Donecopperide positioned in the (h)5-HT<sub>4</sub>R (A) and (h)AChE (B) binding sites from docking studies. The compound and the side chains of the binding site residues are represented by the stick-like shapes, and the protein is represented in ribbon. This figure was made with PYMOL (DeLano Scientific, 2002, San Carlo, U.S.A.).

**Table 4. Pharmacological and Toxicological Properties of Donecopperide**

compound	doses (mg/kg)	LD <sub>50</sub> (mg/kg)	symptoms	
			subtoxic doses	toxic doses
donecopperide	1–10		no symptoms	
	100	75	hypoactivity passivity	convulsions
amphetamine	2		hyperactivity exophthalmic irritability	
chlorpromazine	10		hypotonia ataxia sleep	

while they are both almost devoid of the AChE inhibitory effect. The structure of **19** has been docked into the active site of (h)AChE. While, its conformation appeared to be similar to donecopperide, the rigidity of **19** appears to be strengthened by the mesomeric effect due to its carboxamide group. Consequently, **19**, contrary to donecopperide, seems not able to bind in the same time through its carbonyl group and its piperidine nitrogen atom with Phe<sub>295</sub> and Water<sub>931</sub> of (h)AChE,

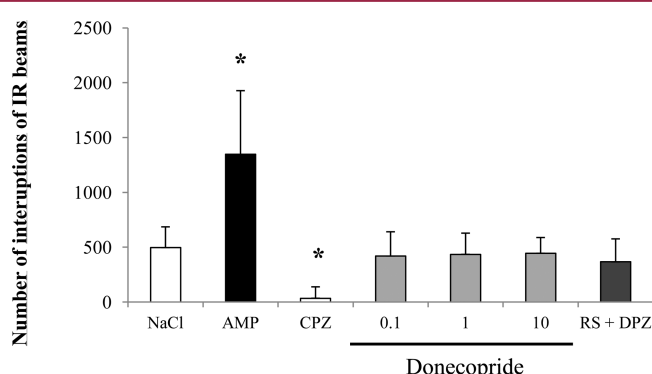


**Figure 5.** Effect of donecopperide on spontaneous locomotor activity. Data are expressed as the mean  $\pm$  standard deviation ( $n = 9\text{--}10$ ). Drugs were administered intraperitoneally (IP) 30 min before placing mice in the actimeter, except for DPZ which was administered subcutaneously (SC) 20 min before the test. Donecopperide: 0.1–10 mg/kg; AMP: amphetamine 2 mg/kg; CPZ: chlorpromazine 10 mg/kg; RS + DPZ: 0.1 mg/kg + DPZ 0.3 mg/kg (\* $p < 0.05$  NaCl, SNK test).

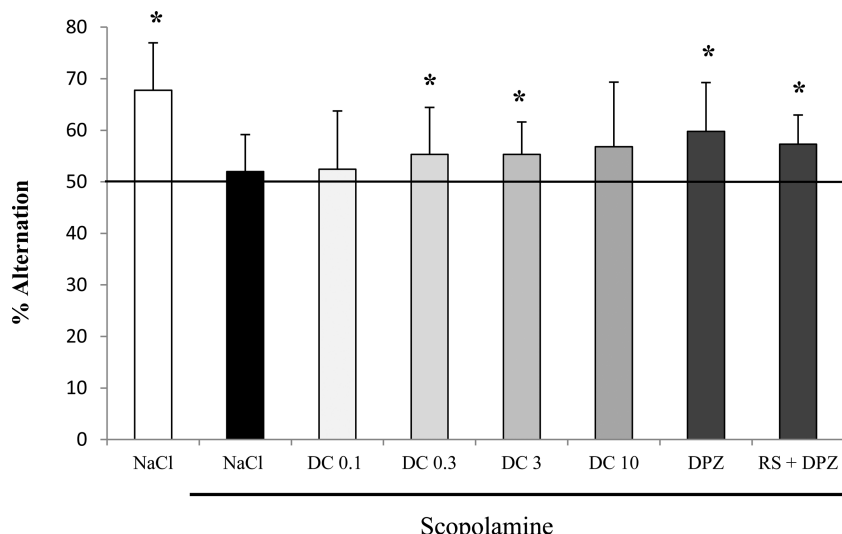


**Figure 6.** Effect of donecoperide on scopolamine-induced impairment during the spontaneous alternation test. Data are expressed as the mean  $\pm$  standard deviation ( $n = 10\text{--}12$ ). Drugs were administered IP 30 min before the test, except for DPZ, and scopolamine was administered SC 30 and 20 min, respectively. DC (donecoperide): 0.1, 0.3, 3, and 10 mg/kg; DPZ: 1 mg/kg; RS + DPZ: 2 0.1 mg/kg + DPZ 0.3 mg/kg; scopolamine: 0.5 mg/kg (\* $p < 0.05$  versus 50%; univariate  $t$  test).

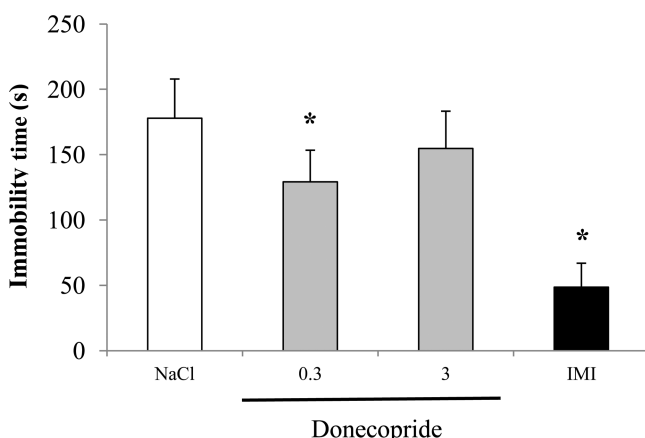


**Figure 7.** Effect of donecoperide on time immobility during the forced swimming test. Data are expressed as the mean  $\pm$  standard deviation ( $n = 10\text{--}12$ ). Drugs were administered IP 30 min before the test. Donecoperide: 0.3, 3 mg/kg; imipramine (IMI) 16 mg/kg (\* $p < 0.05$  NaCl, Student–Newman–Keuls [SNK] test).

respectively (Figure 9). This might also explain the inactivity of **21** against AChE.

In summary, in the structural system derived from **2** as an MTDL hit, 5-HT<sub>4</sub>R affinity seems to be linked to the presence, on the nitrogen atom of the piperidine ring, of a not-too-hindering methylcycloalkyl group, eventually bearing an intracyclic nitrogen. On the other hand, the catalytic AChE inhibition appears to require such a methylcycloalkyl group, but can also be displayed by a benzyl, a methylpyridine, or a methylpiperidine substituent. It is on the basis of these results and considering our objective that we selected compounds **1**, **8**–**10**, and **13** for additional evaluations.

All the tested compounds displayed also high human 5-HT<sub>4</sub>R affinities at  $10^{-8}$  M (Table 2) confirming the relevance of the use (*gp*)5-HT<sub>4</sub>R to select potential (*h*)5-HT<sub>4</sub>R ligands.<sup>65</sup>

Concerning their pharmacological profile, while compounds **1**, **8**, **9**, and **13** were found to be 5-HT<sub>4</sub>R partial agonists (in a similar manner as **2**), compound **10** acted as a very partial

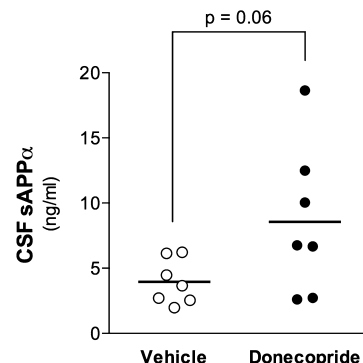


**Figure 8.** Acute in vivo treatment with donecoperide shows a tendency to increase sAPP $\alpha$  release in the CSF of 2-month-old C57BL/6 mice. sAPP $\alpha$  was quantified via enzyme-linked immunosorbent assay (ELISA). Each dot represents an individual mouse; the horizontal lines show the means of each group. The  $p$  value is indicated (unpaired Student's  $t$  test).

agonist. This profile is in accordance with our objective, because prolonged exposure of G protein-coupled receptors to an agonist can result in receptor desensitization, which is often dependent on the degree of intrinsic activity.<sup>66</sup> An opposite relationship seems to have been established between these results and the  $K_{i(5\text{-HT}_4\text{R})}$  values of the tested compounds, since it appears that the higher their affinity, the more partial their agonist effect. This result appears to be concordant with that reported in the literature.<sup>67</sup>

At last, concerning the capacity of the tested compound to displace propidium iodide from the PAS of AChE, compounds **1**, **8**, and **9** acted in a similar manner as DPZ (20%–24%), while **13** displaced propidium less (13%) and **10** displaced it slightly more (30%). The results displayed by **13** and **10** could be correlated in an opposite relation with their  $IC_{50(AChE)}$  values since the most potent AChEI in the series (**13**) weakly interacted with the PAS, while the less potent inhibitor (**10**) interacted more strongly. The weak AChE catalytic inhibitory effect displayed by the latter compound might appear to be inconsistent with its docking in the enzyme-active site. Indeed,

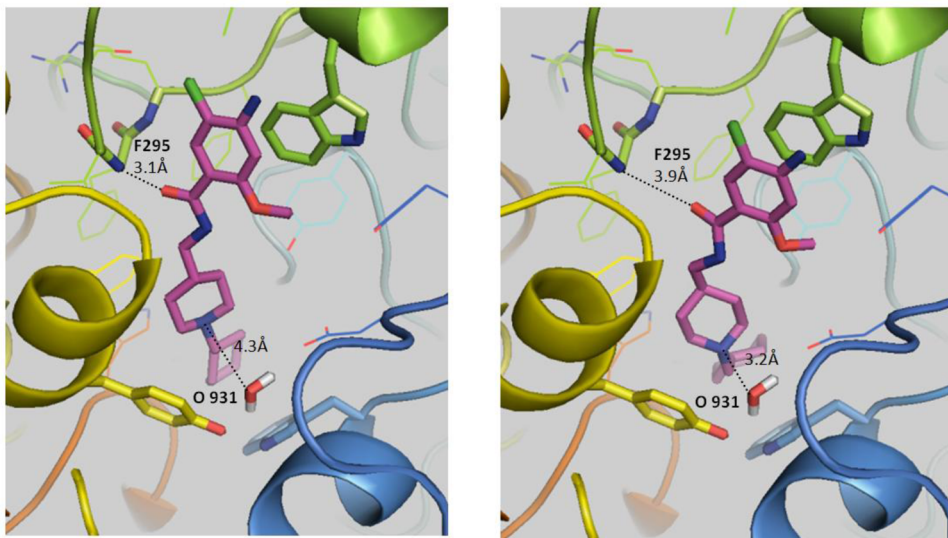


**Figure 9.** Two representative docking poses of compound **19** into (*h*)AChE. The compounds and the side chains of the binding site residues are in stick and the protein in ribbon representation. This figure was made with PYMOL (DeLano Scientific, 2002, San Carlo, U.S.A.).

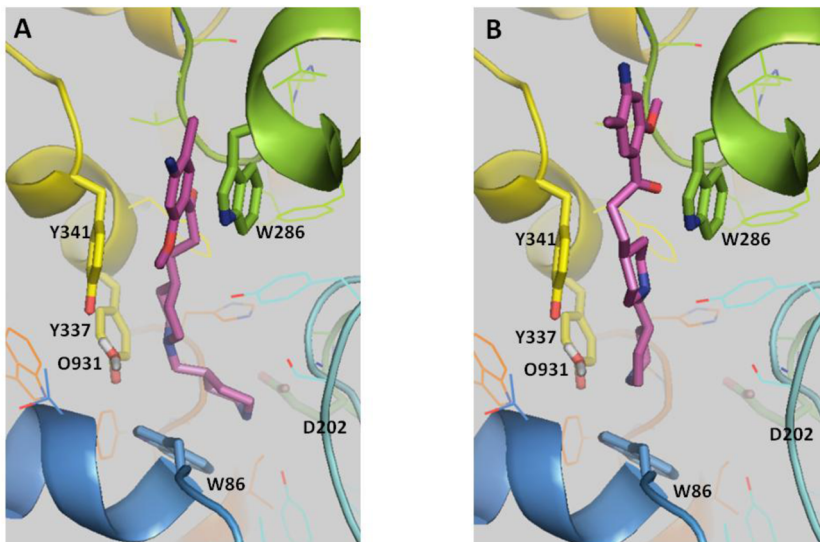


**Figure 10.** Two representative docking poses of compound **10** into (*h*)AChE. The compounds and the side chains of the binding site residues are represented by the stick-like shapes and the protein is represented by ribbon. This figure was made with PYMOL (DeLano Scientific, 2002, San Carlo, U.S.A.).

the cationic nitrogen atom of the middle piperidine ring of **10** (protonated at physiologic pH as well as the nitrogen atom of the terminal piperidine) appears able to bind to the same water molecule as donecoperide (mean ChemPLP Score fit = 104.02). At the same time, the second nitrogen atom on the terminal piperidine ring is located near Glu<sub>202</sub>, which unusually appeared protonated using the ProPKA software (Figure 10A).<sup>68,69</sup> However, in these conditions, a second pose was also generated by the docking study in which it was the terminal piperidine that interacted with the water molecule (mean ChemPLP Score fit = 87.61; see Figure 10B). According to this hypothesis, the phenyl ring of compound **10** covers more Trp<sub>286</sub> whereas its interaction with Trp<sub>86</sub> would be weaker. Despite the lower score, the second pose seems to be in better agreement with experimental results, as it features the worst binding affinity and the greatest propidium displacement for compound **10** with respect to donecoperide.

Concerning *in vivo* investigations, we have shown that donecoperide has an antiamnesiant effect in a scopolamine-induced deficit model of working memory. Together with our previous results showing the positive effect of donecoperide in recognition memory performance in mice<sup>58</sup> (testing recognition memory), this result confirms the high therapeutic potential of this molecule in the treatment of the cognitive disorders associated with AD. Of note, with respect to the dose (0.3 mg/kg) that revealed a beneficial effect on the two memory and behavioral tests (antiamnesiant and promnesiant effects), an interesting additional antidepressant-like effect was demonstrated. Furthermore, these behavioral effects were associated with an increased release of the neuroprotective sAPP $\alpha$  fragment. Such observations are in agreement with data from the literature, showing, for instance, better memory performance in transgenic mice that overexpress MMP9, which consequently display an increased secretion of sAPP $\alpha$ .<sup>70</sup>

Herein, we were only able to highlight a tendency of an increased release of the nonamyloidogenic APP fragment in the CSF 90 min following a systemic injection. However, that sAPP $\alpha$  increased upon 5-HT<sub>4</sub>R activation is transient,<sup>71</sup> and it is consequently highly difficult to catch the peak of sAPP $\alpha$  in CSF. Kinetics studies using different collection times or intracerebral microdialysis would be necessary to precisely determine the acute action of donecopride in living animals. Moreover, it should be interesting to monitor ACh levels, sAPP $\alpha$ , and A $\beta$  in the CSF or in the brain tissue at the same time. Chronic administration of 5-HT<sub>4</sub>R agonists reduces amyloid pathology and prevents cognitive deficits in AD mouse models.<sup>71,72</sup> Further experiments exploring chronic treatments of AD transgenic mice with donecopride, in comparison with DPZ and pure 5-HT<sub>4</sub>R agonists, would produce valuable insights regarding the potential of donecopride to exert a disease-modifying effect.

## CONCLUSION

In conclusion, we have developed a novel series of MTDL that displayed both DBS AChE inhibitory effects and partial 5-HT<sub>4</sub>R agonist activity *in vitro* in nanomolar ranges. Donecopride, which appears to be the lead of this family, further exhibited *in vivo* procognitive and antiamnesic effects in NMRI mice, and it also appeared able to promote the release of sAPP $\alpha$  in C57BL/6 mice *in vivo*. These results, which appear to gather in a single compound both the activities of DPZ and 2, seem likely to confer a symptomatic and disease-modifying effect to donecopride, thus designing it as a potentially promising drug candidate in AD.

## EXPERIMENTAL SECTION

**Chemistry. General Material and Methods.** All chemical reagents and solvents were purchased from commercial sources and used without further purification. Melting points were determined on a Kofler melting point apparatus. <sup>1</sup>H and <sup>13</sup>C NMR spectra were recorded on a BRUKER AVANCE III 400 MHz with chemical shifts expressed in parts per million (in chloroform-*d*, methanol-*d*<sub>4</sub>, or DMSO-*d*<sub>6</sub>) downfield from TMS as an internal standard and coupling in Hertz. IR spectra were recorded on a PerkinElmer BX FT-IR apparatus using KBr pellets. High-resolution mass spectra (HRMS) were obtained by impact electronic on a Jeol JMS GC Mate spectrometer (compound 1) or by electrospray on a Bruker maXis (compounds 4, 7, 8, 13–19) or on a Q-ToF micro Waters (compounds 6, 9–12, 21). The purities of all tested compounds were analyzed by LC–MS, with the purity all being higher than 95%. Analyses were performed using a Waters Alliance 2695 as separating module (column XBridge C18 2.5  $\mu$ M/4.6  $\times$  50 mM) using the following gradients: A (95%)/B (5%) to A (5%)/B (95%) in 4.00 min. This ratio was held for 1.50 min before returning to initial conditions in 0.50 min. Initial conditions were then maintained for 2.00 min (A = H<sub>2</sub>O, B = CH<sub>3</sub>CN; each containing HCOOH: 0.1%). MS were obtained on a SQ detector by positive ESI.

**General Procedure for the Deprotection and N-Alkylation of *tert*-Butyl 4-[3-(4-amino-5-chloro-2-methoxyphenyl)-3-oxo-propyl]piperidine-1-carboxylate (5) (1; 6–9; 11–15; 17).** *tert*-Butyl 4-[3-(4-amino-5-chloro-2-methoxyphenyl)-3-oxo-propyl]piperidine-1-carboxylate 5 was dissolved in DCM/TFA (1/1). The mixture was then stirred 15 min at rt. After concentration under reduced pressure, the resulting intermediate was dissolved in DMF or 1,4-dioxane (for compounds 13–15). K<sub>2</sub>CO<sub>3</sub> (10 equiv) and halogenoalkyle (1.3 equiv) were added, and the mixture was warmed to 110 °C for 4 h. After cooling, DCM was added, and the mixture was washed 4 times with brine. The organic layer was then dried over MgSO<sub>4</sub>, filtered, and evaporated under reduced pressure. The crude residue was purified on

deactivated silica gel (gradient of elution: DCM to DCM/MeOH (98/2)).

**1-(4-Amino-5-chloro-2-methoxyphenyl)-3-[1-(cyclohexylmethyl)-4-piperidyl]propan-1-one (1).**<sup>58</sup> Pale yellow powder (44%): mp 153–155 °C; <sup>1</sup>H NMR (400 MHz, CDCl<sub>3</sub>):  $\delta$  7.79 (s, 1H), 6.48 (s, 1H), 4.44 (br s, 2H), 3.85 (s, 3H), 2.89 (m, 2H), 2.84 (m, 2H), 2.08 (d, *J* = 6.8 Hz, 2H), 1.68 (m, 11H), 1.47 (m, 1H), 1.20 (m, 6H), 0.85 (m, 2H); <sup>13</sup>C NMR (100 MHz, CDCl<sub>3</sub>):  $\delta$  199.3, 159.5, 147.7, 132.2, 119.0, 111.2, 97.6, 66.3, 55.6, 54.5 (2C), 41.0, 35.8, 35.3, 32.3 (2C), 32.2 (2C), 31.4, 26.8, 26.2 (2C); LC-MS: [M + H]<sup>+</sup> = 393.58–395.59; IR (KBr):  $\nu$  cm<sup>−1</sup> 3485, 3330, 2921, 2850, 1641, 1623, 1575, 1452, 1421, 1214, 1177; HRMS (*m/z*) calcd for C<sub>22</sub>H<sub>33</sub>ClN<sub>2</sub>O<sub>2</sub> [M]<sup>+</sup> 392.22303, found 392.22399.

**Ethyl 3-(4-amino-5-chloro-2-methoxyphenyl)-3-oxopropanoate (4).** To a suspension of 4-amino-5-chloro-2-methoxybenzoic acid (603 mg, 2.99 mmol) in dry THF (30 mL) was added portion-wise CDI (533 mg, 3.29 mmol). The mixture was stirred at rt for 6 h and, then, potassium 3-ethoxy-3-oxopropanoate (611 mg, 3.59 mmol) and MgCl<sub>2</sub> (342 mg, 3.59 mmol) were added portion-wise. The mixture was stirred at 40 °C for 2 days. After evaporation of the solvent, the residue was diluted with DCM, washed successively with water, saturated aqueous NaHCO<sub>3</sub> and brine, dried over MgSO<sub>4</sub>, and evaporated in vacuo. The residue was then purified on silica gel (gradient of elution: CH<sub>3</sub>AcOEt 8/2 to 7/3) to afford 603 mg of product. White powder (62%): mp 124 °C; <sup>1</sup>H NMR (400 MHz, CDCl<sub>3</sub>):  $\delta$  7.92 (s, 1H), 6.23 (s, 1H), 4.56 (br s, 2H), 4.17 (qd, *J* = 7.3 Hz, 2H), 3.87 (s, 2H), 3.82 (s, 3H), 1.24 (t, *J* = 7.3 Hz, 3H); <sup>13</sup>C NMR (100 MHz, CDCl<sub>3</sub>):  $\delta$  189.6, 168.6, 159.9, 148.7, 132.5, 117.3, 111.6, 97.0, 60.8, 55.4, 50.5, 14.2; LC-MS: [M + H]<sup>+</sup> = 272.43–274.43; IR (KBr):  $\nu$  cm<sup>−1</sup> 3463, 3362, 3323, 2983, 1725, 1648, 1622, 1573, 1469, 1423, 1326, 1262, 1221, 1155; HRMS (*m/z*) calcd for C<sub>12</sub>H<sub>15</sub>ClNO<sub>4</sub> [M + H]<sup>+</sup> 272.068412, found 272.068374.

**tert-Butyl 4-(3-(4-amino-5-chloro-2-methoxyphenyl)-3-oxopropyl)piperidine-1-carboxylate (5).**<sup>73</sup> To a solution of compound 3 (2.3 g, 8.5 mmol) in DMF (20 mL) were added *tert*-butyl 4-(iodomethyl)piperidine-1-carboxylate (3.05 g, 9.5 mmol) and K<sub>2</sub>CO<sub>3</sub> (2.3 g, 17.1 mmol). The mixture was stirred at rt for 48 h. The reaction mixture was diluted with water, and the product was extracted with AcOEt. Combined organic layer was washed with water and brine and then dried over MgSO<sub>4</sub>. Evaporation of the solvent gave a crude mixture (4.8 g, 10.3 mmol), which was directly dissolved in EtOH (500 mL). H<sub>2</sub>O (100 mL) and KOH (2.65 g, 47.3 mmol) were added to the solution. The reaction mixture was refluxed for 3 h. EtOH was then evaporated, and the resulting residue was diluted with H<sub>2</sub>O and extracted with AcOEt. The organic layer was washed with H<sub>2</sub>O and brine. Evaporation of the solvent provided a crude product, which was purified by column on silica (gradient of elution: DCM to DCM/AcOEt 6/4) to provide compound 2 (2.9 g). White powder (86%): mp 135–137 °C; <sup>1</sup>H NMR (400 MHz, CDCl<sub>3</sub>):  $\delta$  7.71 (s, 1H), 6.23 (s, 1H), 4.63 (br s, 2H), 4.01 (m, 2H), 3.76 (s, 3H), 2.84 (t, *J* = 7.5 Hz, 2H), 2.61 (m, 2H), 1.61 (m, 2H), 1.53 (m, 2H), 1.39 (s, 9H), 1.35 (m, 1H), 1.03 (m, 2H); <sup>13</sup>C NMR (100 MHz, CDCl<sub>3</sub>):  $\delta$  198.7, 159.5, 154.8, 148.0, 131.9, 118.3, 111.0, 97.3, 79.1, 55.5, 43.8 (2C), 40.5, 35.6, 31.9 (2C), 31.0, 28.3 (3C); LC-MS: [M + H]<sup>+</sup> = 397.60–399.60; IR (KBr):  $\nu$  cm<sup>−1</sup> 3470, 3353, 2975, 2930, 2851, 1673, 1624, 1588, 1421, 1366, 1311, 1250, 1216.

**1-(4-Amino-5-chloro-2-methoxyphenyl)-3-[1-(cyclopropylmethyl)-4-piperidyl]propan-1-one (6).** Pale yellow powder (38%): mp 161–163 °C; <sup>1</sup>H NMR (400 MHz, CDCl<sub>3</sub>):  $\delta$  7.75 (s, 1H), 6.23 (s, 1H), 4.46 (s, 2H), 3.81 (s, 3H), 3.03 (m, 2H), 2.87 (m, 2H), 2.19 (d, *J* = 6.8 Hz, 2H), 1.88 (m, 2H), 1.67 (m, 2H), 1.56 (m, 2H), 1.32 (m, 1H), 1.27 (m, 2H), 0.83 (m, 1H), 0.47 (m, 2H), 0.06 (m, 2H); <sup>13</sup>C NMR (100 MHz, CDCl<sub>3</sub>):  $\delta$  199.2, 159.5, 147.7, 132.2, 118.9, 111.2, 97.5, 64.2, 55.6, 54.0 (2C), 40.9, 35.6, 32.2 (2C), 31.4, 8.5, 4.0 (2C); LC-MS: [M + H]<sup>+</sup> = 351.49–353.45; IR (KBr):  $\nu$  cm<sup>−1</sup> 3466, 3350, 2924, 2849, 1644, 1621, 1586, 1465, 1420, 1215, 1178; HRMS (*m/z*) calcd for C<sub>19</sub>H<sub>28</sub>ClN<sub>2</sub>O<sub>2</sub> [M + H]<sup>+</sup> 351.1839, found 351.1841.

**1-(4-Amino-5-chloro-2-methoxyphenyl)-3-[1-(cyclobutylmethyl)-4-piperidyl]propan-1-one (7).** Yellow powder (45%): mp 142–144 °C; <sup>1</sup>H NMR (400 MHz, CDCl<sub>3</sub>):  $\delta$  7.77 (s, 1H), 6.25 (s, 1H), 4.41

(br s, 2H), 3.84 (s, 3H), 2.88 (t,  $J = 8.0$  Hz, 2H), 2.81 (m, 2H), 2.54 (m, 1H), 2.37 (d,  $J = 6.6$  Hz, 2H), 2.06 (m, 2H), 1.78 (m, 8H), 1.57 (m, 2H), 1.25 (m, 3H);  $^{13}\text{C}$  NMR (100 MHz,  $\text{CDCl}_3$ ):  $\delta$  199.1, 159.4, 147.6, 132.2, 118.9, 111.2, 97.5, 65.9, 55.6, 54.0 (2C), 40.9, 35.4, 34.2, 32.2 (2C), 31.3, 28.3 (2C), 18.8; LC-MS:  $[\text{M} + \text{H}]^+ = 365.53 - 367.54$ ; IR (KBr):  $\nu$   $\text{cm}^{-1}$  3485, 3327, 2923, 2852, 1642, 1624, 1575, 1453, 1421, 1214, 1175; HRMS ( $m/z$ ) calcd for  $\text{C}_{20}\text{H}_{30}\text{ClN}_2\text{O}_2$   $[\text{M} + \text{H}]^+$  365.199032, found 365.198665.

**1-(4-Amino-5-chloro-2-methoxyphenyl)-3-[1-(cyclopentylmethyl)-4-piperidyl]propan-1-one (8).** Yellow powder (35%): mp 141–143 °C;  $^1\text{H}$  NMR (400 MHz,  $\text{CDCl}_3$ ):  $\delta$  7.79 (s, 1H), 6.26 (s, 1H), 4.44 (br s, 2H), 3.85 (s, 3H), 2.90 (m, 4H), 2.24 (d,  $J = 7.1$  Hz, 2H), 2.05 (m, 1H), 1.86 (m, 2H), 1.76 (m, 2H), 1.60 (m, 6H), 1.50 (m, 2H), 1.21 (m, 5H);  $^{13}\text{C}$  NMR (100 MHz,  $\text{CDCl}_3$ ):  $\delta$  199.2, 159.4, 147.5, 132.2, 119.0, 111.2, 97.5, 65.2, 55.6, 54.3 (2C), 40.9, 37.5, 35.7, 32.2 (2C), 31.8 (2C), 31.3, 25.2 (2C); LC-MS:  $[\text{M} + \text{H}]^+ = 379.57 - 381.56$ ; IR (KBr):  $\nu$   $\text{cm}^{-1}$  3486, 3332, 2924, 2860, 1644, 1623, 1574, 1453, 1422, 1214, 1175; HRMS ( $m/z$ ) calcd for  $\text{C}_{21}\text{H}_{32}\text{ClN}_2\text{O}_2$   $[\text{M} + \text{H}]^+$  379.214682, found 379.214484.

**1-(4-Amino-5-chloro-2-methoxyphenyl)-3-[1-(cycloheptylmethyl)-4-piperidyl]propan-1-one (9).** Yellow powder (42%): mp 147–149 °C;  $^1\text{H}$  NMR (400 MHz,  $\text{CDCl}_3$ ):  $\delta$  7.78 (s, 1H), 6.27 (s, 1H), 4.49 (br s, 2H), 3.85 (s, 3H), 2.87 (m, 2H), 2.81 (m, 2H), 2.02 (d,  $J = 7.3$  Hz, 2H), 1.57 (m, 17H), 1.22 (m, 3H), 1.08 (m, 2H);  $^{13}\text{C}$  NMR (100 MHz,  $\text{CDCl}_3$ ):  $\delta$  198.2, 158.5, 146.7, 131.2, 117.8, 110.2, 96.5, 65.3, 54.6, 53.3 (2C), 39.9, 35.4, 34.6, 31.9 (2C), 31.0 (2C), 30.3, 27.5 (2C), 25.5 (2C); LC-MS:  $[\text{M} + \text{H}]^+ = 407.53 - 409.52$ ; IR (KBr):  $\nu$   $\text{cm}^{-1}$  3481, 3247, 2920, 2850, 1638, 1622, 1582, 1454, 1419, 1214, 1176; HRMS ( $m/z$ ) calcd for  $\text{C}_{23}\text{H}_{36}\text{ClN}_2\text{O}_2$   $[\text{M} + \text{H}]^+$  407.2465, found 407.2461.

**1-(4-Amino-5-chloro-2-methoxyphenyl)-3-[1-(4-piperidylmethyl)-4-piperidyl]propan-1-one dihydrochloride (10).** Following the previous general procedure, the intermediate *tert*-butyl 4-[[4-[3-(4-amino-5-chloro-2-methoxyphenyl)-3-oxo-propyl]-1-piperidyl]methyl]piperidine-1-carboxyl ate is obtained. Pale yellow powder (24%): mp 78–80 °C;  $^1\text{H}$  NMR (400 MHz,  $\text{CDCl}_3$ ):  $\delta$  7.76 (s, 1H), 6.23 (s, 1H), 4.44 (br s, 2H), 4.03 (m, 2H), 3.82 (s, 3H), 2.87 (t,  $J = 7.8$  Hz, 2H), 2.80 (m, 2H), 2.65 (m, 2H), 2.10 (d,  $J = 6.8$  Hz, 2H), 1.83 (m, 2H), 1.58 (m, 7H), 1.41 (s, 9H), 1.23 (m, 3H), 1.03 (m, 2H);  $^{13}\text{C}$  NMR (100 MHz,  $\text{CDCl}_3$ ):  $\delta$  199.1, 159.5, 155.0, 147.6, 132.3, 119.0, 111.3, 97.6, 79.2, 65.1, 55.7, 54.6 (2C), 43.8 (2C), 40.9, 35.7, 33.8, 32.3 (2C), 31.3, 30.9 (2C), 28.4 (3C); LC-MS:  $[\text{M} + \text{H}]^+ = 494.53 - 496.55$ ,  $[\text{M} + \text{H} - \text{BOC}]^+ = 394.49 - 396.48$ ; IR (KBr):  $\nu$   $\text{cm}^{-1}$  3479, 3347, 2922, 2850, 1688, 1674, 1622, 1587, 1466, 1452, 1247, 1215, 1175; HRMS ( $m/z$ ) calcd for  $\text{C}_{26}\text{H}_{40}\text{ClN}_3\text{O}_4$   $[\text{M} + \text{H}]^+$  494.2786, found 494.2766. To a solution of *tert*-butyl 4-[[4-[3-(4-amino-5-chloro-2-methoxyphenyl)-3-oxo-propyl]-1-piperidyl]methyl]piperidine-1-carboxylate (40 mg, 0.09 mmol) in EtOH (2 mL) was added HCl 37% (300  $\mu\text{L}$ ). The mixture was stirred at rt for 3 h and then concentrated under reduced pressure. The residue was then stirred into  $\text{Et}_2\text{O}$  and filtered to afford 30 mg of compound 9. Yellow powder (80%): mp >260 °C;  $^1\text{H}$  NMR (400 MHz,  $\text{DMSO}-d_6$ ):  $\delta$  10.23 (br s, 1H), 9.09 (br s, 1H), 8.96 (br s, 1H), 7.53 (s, 1H), 6.46 (s, 1H), 3.99 (s, 3H), 3.45 (m, 2H), 3.22 (m, 2H), 2.91 (m, 2H), 2.81 (m, 6H), 2.11 (m, 1H), 1.96 (m, 2H), 1.76 (m, 2H), 1.63 (m, 2H), 1.46 (m, 3H), 1.38 (m, 2H);  $^{13}\text{C}$  NMR (100 MHz,  $\text{DMSO}-d_6$ ):  $\delta$  196.6, 159.6, 150.1, 131.1, 115.8, 109.3, 97.1, 60.4, 55.6, 52.3 (2C), 42.3 (2C), 39.7, 32.7, 30.2, 28.4 (2C), 28.3, 26.6 (2C); LC-MS:  $[\text{M} + \text{H}]^+ = 394.38 - 396.42$ ; IR (KBr):  $\nu$   $\text{cm}^{-1}$  3390, 3296, 3194, 2938, 2732, 1660, 1625, 1593, 1449, 1417, 1212, 1180; HRMS ( $m/z$ ) calcd for  $\text{C}_{21}\text{H}_{33}\text{ClN}_3\text{O}_2$   $[\text{M} + \text{H}]^+$  394.2261, found 394.2269.

**1-(4-Amino-5-chloro-2-methoxyphenyl)-3-[1-(cyclohexylethyl)-4-piperidyl]propan-1-one (11).** Yellow powder (40%): mp 169–171 °C;  $^1\text{H}$  NMR (400 MHz,  $\text{CDCl}_3$ ):  $\delta$  7.76 (s, 1H), 6.23 (s, 1H), 4.42 (br s, 2H), 3.82 (s, 3H), 2.89 (m, 4H), 2.28 (m, 2H), 1.84 (m, 2H), 1.61 (m, 9H), 1.36 (m, 2H), 1.20 (m, 7H), 0.90 (m, 2H);  $^{13}\text{C}$  NMR (100 MHz,  $\text{CDCl}_3$ ):  $\delta$  199.1, 159.5, 147.6, 132.2, 118.9, 111.2, 97.5, 57.0, 55.6, 54.0 (2C), 40.8, 36.5, 35.5, 34.4, 33.4 (2C), 32.0 (2C), 31.2, 26.6, 26.3 (2C); LC-MS:  $[\text{M} + \text{H}]^+ = 407.41 - 409.52$ ; IR (KBr):  $\nu$   $\text{cm}^{-1}$  3486, 3324, 2918, 2847, 1637, 1621, 1571, 1453, 1304, 1212,

1173; HRMS ( $m/z$ ) calcd for  $\text{C}_{23}\text{H}_{36}\text{ClN}_2\text{O}_2$   $[\text{M} + \text{H}]^+$  407.2465, found 407.2468.

**1-(4-Amino-5-chloro-2-methoxyphenyl)-3-[1-(2-methylcyclohexyl)methyl]-4-piperidyl propan-1-one (12).** Powder (49%):  $^1\text{H}$  NMR (400 MHz,  $\text{CDCl}_3$ ):  $\delta$  7.75 (s, 1H, 1H\*), 6.23 (s, 1H, 1H\*), 4.43 (br s, 2H, 2H\*), 3.81 (s, 3H, 3H\*), 2.87 (m, 2H, 3H\*), 2.81 (m, 2H), 2.74 (m, 1H\*), 2.32 (dd,  $J = 11.8$  Hz,  $J = 3.2$  Hz, 1H\*), 2.06 (m, 2H), 2.00 (m, 1H\*), 1.92 (m, 1H\*), 1.81 (m, 3H), 1.60 (m, 7H, 11H\*), 1.38 (m, 6H, 3H\*), 1.21 (m, 3H, 4H\*), 0.87 (d,  $J = 5.8$  Hz, 3H\*), 0.80 (d,  $J = 7.1$  Hz, 3H);  $^{13}\text{C}$  NMR (100 MHz,  $\text{CDCl}_3$ ):  $\delta$  199.3 (C, C\*), 159.5 (C, C\*), 147.6 (C, C\*), 132.2 (C, C\*), 119.0 (C, C\*), 111.3 (C, C\*), 97.6 (C, C\*), 63.7 (C\*), 62.0 (C), 56.1 (C\*), 55.7 (C, C\*), 54.8 (C), 54.5 (C), 53.2 (C\*), 41.0 (C), 41.0 (C\*), 37.2 (C, C\*), 36.6 (C\*), 35.9 (C), 35.9 (C\*), 33.0 (C), 32.4 (2C\*), 32.4 (2C), 32.3 (C\*), 31.5 (C\*), 31.4 (C), 31.0 (C), 26.4 (C\*), 26.4 (C), 26.3 (C\*), 25.6 (C), 21.9 (C, C\*), 20.5 (C\*), 13.6 (C); LC-MS:  $[\text{M} + \text{H}]^+ = 407.54 - 409.63$ ; HRMS ( $m/z$ ) calcd for  $\text{C}_{23}\text{H}_{36}\text{ClN}_2\text{O}_2$   $[\text{M} + \text{H}]^+$  407.2465, found 407.2458. The ratio of these 2 diastereoisomers was obtained in proportions 3/1\* according to the  $^1\text{H}$  NMR spectra.

**1-(4-Amino-5-chloro-2-methoxyphenyl)-3-(1-benzyl)-4-piperidyl propan-1-one (13).** Pale yellow oil (23%);  $^1\text{H}$  NMR (400 MHz,  $\text{CDCl}_3$ ):  $\delta$  7.71 (s, 1H), 7.19 (m, 5H), 6.18 (s, 1H), 4.39 (s, 2H), 3.76 (s, 3H), 3.45 (s, 2H), 2.81 (m, 4H), 1.90 (br t,  $J = 10.2$  Hz, 2H), 1.61 (br d,  $J = 9.2$  Hz, 2H), 1.52 (q,  $J = 6.9$  Hz, 2H), 1.22 (m, 3H);  $^{13}\text{C}$  NMR (100 MHz,  $\text{CDCl}_3$ ):  $\delta$  199.2, 159.5, 147.7, 137.7, 132.3, 129.5 (2C), 128.2 (2C), 127.1, 118.9, 111.3, 97.5, 63.3, 55.6, 53.7 (2C), 40.8, 35.4, 31.9 (2C), 31.4; HRMS ( $m/z$ ) calcd for  $\text{C}_{22}\text{H}_{28}\text{ClN}_2\text{O}_2$   $[\text{M} + \text{H}]^+$  387.183382, found 387.183120.

**1-(4-Amino-5-chloro-2-methoxyphenyl)-3-[1-(3-pyridylmethyl)-4-piperidyl]propan-1-one (14).** Pale yellow oil (40%);  $^1\text{H}$  NMR (400 MHz,  $\text{CDCl}_3$ ):  $\delta$  8.51 (d,  $J = 2.0$  Hz, 1H), 8.50 (dd,  $J = 1.6, 4.8$  Hz, 1H), 7.78 (s, 1H), 7.69 (dt,  $J = 1.6, 7.6$  Hz, 1H), 7.25 (dd,  $J = 4.8, 8.0$  Hz, 1H), 6.25 (s, 1H), 4.48 (s, 2H), 3.83 (s, 3H), 2.87 (m, 4H), 1.99 (br t,  $J = 10.2$  Hz, 2H), 1.68 (br d,  $J = 9.2$  Hz, 2H), 1.68 (br d,  $J = 9.2$  Hz, 2H), 1.58 (q,  $J = 6.9$  Hz, 2H), 1.24 (m, 3H);  $^{13}\text{C}$  NMR (100 MHz,  $\text{CDCl}_3$ ):  $\delta$  199.3, 159.7, 150.7, 148.8, 147.9, 137.2, 133.7, 132.4, 123.6, 119.0, 111.4, 97.7, 60.5, 55.7, 53.8 (2C), 40.9, 35.4, 32.0 (2C), 31.2; HRMS ( $m/z$ ) calcd for  $\text{C}_{21}\text{H}_{27}\text{ClN}_3\text{O}_2$   $[\text{M} + \text{H}]^+$  388.178631, found 388.178595.

**1-(4-Amino-5-chloro-2-methoxyphenyl)-3-[1-(4-pyridylmethyl)-4-piperidyl]propan-1-one (15).** Pale yellow oil (45%);  $^1\text{H}$  NMR (400 MHz,  $\text{CDCl}_3$ ):  $\delta$  8.52 (d,  $J = 6.0$  Hz, 2H), 7.78 (s, 1H), 7.26 (d,  $J = 6.0$  Hz, 2H), 6.25 (s, 1H), 4.50 (s, 2H), 3.83 (s, 3H), 3.47 (s, 2H), 2.89 (t,  $J = 7.6$  Hz, 2H), 2.83 (br d,  $J = 11.2$  Hz, 2H), 1.97 (br t,  $J = 10.8$  Hz, 2H), 1.68 (br d,  $J = 9.2$  Hz, 2H), 1.59 (q,  $J = 6.9$  Hz, 2H), 1.26 (m, 3H);  $^{13}\text{C}$  NMR (100 MHz,  $\text{CDCl}_3$ ):  $\delta$  199.3, 159.7, 149.8 (2C), 148.2, 147.9, 132.4, 124.2 (2C), 119.0, 111.4, 97.6, 62.2, 55.7, 54.1 (2C), 40.9, 35.4, 32.2 (2C), 31.3; HRMS ( $m/z$ ) calcd for  $\text{C}_{21}\text{H}_{27}\text{ClN}_3\text{O}_2$   $[\text{M} + \text{H}]^+$  388.178631, found 388.178502.

**General Procedure for the Preparation of Oximes (16–17).** To a solution of compound 1 in pyridine was added alkoxyamine hydrochloride (3.6 equiv) in 3 portions every 2 h. The mixture was stirred at rt for 24 h. After dilution with water, the aqueous layer was extracted 3 times with AcOEt. The organic layers were combined, washed 5 times with brine, dried over  $\text{MgSO}_4$ , and concentrated under reduced pressure. The crude residue was purified on deactivated silica gel (gradient: DCM to DCM/AcOEt (9/1)) to provide the desired product.

**(E)-1-(4-Amino-5-chloro-2-methoxyphenyl)-3-[1-(cyclohexylmethyl)-4-piperidyl]propan-1-one oxime (16).** White powder (35%): mp 194–196 °C;  $^1\text{H}$  NMR (400 MHz,  $\text{CD}_3\text{OD}$ ):  $\delta$  6.99 (s, 1H), 6.47 (s, 1H), 3.75 (s, 3H), 2.93 (m, 2H), 2.71 (m, 2H), 2.23 (d,  $J = 6.8$  Hz, 2H), 2.02 (m, 2H), 1.72 (m, 8H), 1.55 (m, 1H), 1.28 (m, 7H), 0.93 (m, 2H);  $^{13}\text{C}$  NMR (100 MHz,  $\text{CD}_3\text{OD}$ ):  $\delta$  159.8, 157.3, 145.9, 129.8, 115.8, 109.4, 98.2, 65.4, 54.6, 53.9 (2C), 35.2, 34.4, 31.8, 31.6 (2C), 30.8 (2C), 26.1, 25.7 (2C), 25.3; IR (KBr):  $\nu$   $\text{cm}^{-1}$  3368, 2925, 2850, 2815, 1620, 1508, 1461, 1449, 1412, 1336, 1254, 1214, 992; LC-MS:  $[\text{M} + \text{H}]^+ = 408.53 - 410.51$ ; HRMS ( $m/z$ ) calcd for  $\text{C}_{22}\text{H}_{35}\text{ClN}_3\text{O}_2$   $[\text{M} + \text{H}]^+$  408.241231, found 408.240998.

**2-Chloro-4-[*(E*)-C-[2-[1-(cyclohexylmethyl)-4-piperidyl]ethyl]-N-methoxy-carbon-imidoyl]-5-methoxyaniline (17).** Yellow oil (42%);  $^1\text{H}$  NMR (400 MHz,  $\text{CDCl}_3$ ):  $\delta$  7.12 (s, 1H), 6.25 (s, 1H), 4.10 (br s, 2H), 3.89 (s, 3H), 3.72 (s, 3H), 2.79 (m, 2H), 2.63 (m, 2H), 2.04 (d,  $J$  = 6.8 Hz, 2H), 1.65 (m, 9H), 1.44 (m, 1H), 1.22 (m, 8H), 0.83 (m, 2H);  $^{13}\text{C}$  NMR (100 MHz,  $\text{CDCl}_3$ ):  $\delta$  159.9, 157.1, 144.2, 130.4, 117.0, 110.5, 98.5, 66.2, 61.5, 55.5, 54.5 (2C), 36.1, 35.2, 32.4, 32.1 (2C), 32.0 (2C), 29.7, 26.5, 26.2 (2C); LC-MS:  $[\text{M} + \text{H}]^+ = 422.54 - 424.53$ ; IR (KBr):  $\nu$   $\text{cm}^{-1}$  2921, 2850, 1621, 1506, 1464, 1450, 1411, 1338, 1258, 1213, 1051; HRMS ( $m/z$ ) calcd for  $\text{C}_{23}\text{H}_{38}\text{ClN}_3\text{O}_2$   $[\text{M} + \text{H}]^+$  422.256882, found 422.256616.

**1-(4-Amino-5-chloro-2-methoxyphenyl)-3-[1-(cyclohexylmethyl)-4-piperidyl]propan-1-ol (18).** To a solution of compound **1** (33 mg, 0.084 mmol) in MeOH was added  $\text{NaBH}_4$  (25 mg, 0.673 mmol). The mixture was stirred for 3 h. After concentration, the residue was dissolved in DCM, washed with brine, dried over  $\text{MgSO}_4$ , and then evaporated under reduced pressure. The crude product was purified on deactivated silica gel (gradient of elution: DCM to DCM/MeOH) to afford 20 mg of desired product. Pale yellow powder (62%): mp: 136–138  $^\circ\text{C}$ ;  $^1\text{H}$  NMR (400 MHz,  $\text{CDCl}_3$ ):  $\delta$  7.12 (s, 1H), 6.26 (s, 1H), 4.69 (dd,  $J$  = 7.5 Hz,  $J$  = 5.8 Hz, 1H), 4.00 (br s, 2H), 3.75 (s, 3H), 2.82 (m, 2H), 2.06 (d,  $J$  = 7.0 Hz, 2H), 1.79 (m, 2H), 1.67 (m, 10H), 1.45 (m, 1H), 1.36 (m, 1H), 1.19 (m, 6H), 0.83 (m, 2H);  $^{13}\text{C}$  NMR (100 MHz,  $\text{CDCl}_3$ ):  $\delta$  156.2, 142.5, 127.5, 124.0, 110.6, 98.8, 70.0, 66.2, 55.4, 54.5 (2C), 35.8, 35.2, 34.4, 32.9, 32.3 (2C), 32.1 (2C), 26.8, 26.2 (2C); IR (KBr):  $\nu$   $\text{cm}^{-1}$  3393, 2920, 2850, 1622, 1580, 1504, 1466, 1412, 1209; LC-MS:  $[\text{M} + \text{H}]^+ = 395.64 - 397.64$ . HRMS ( $m/z$ ) calcd for  $\text{C}_{22}\text{H}_{37}\text{ClN}_2\text{O}_2$   $[\text{M} + \text{H}]^+$  395.245983, found 395.245734.

**4-Amino-5-chloro-N-[1-(cyclohexylmethyl)-4-piperidyl]methyl]-2-methoxybenzamide (19).** Following the previous general procedure used for the deprotection and N-alkylation of **5**, **19** is obtained starting from *tert*-butyl 4-[(4-amino-5-chloro-2-methoxybenzoyl)amino]-methyl] piperidine-1-carboxylate (**20**). White powder (38%): mp 154–156  $^\circ\text{C}$ ;  $^1\text{H}$  NMR (400 MHz,  $\text{CDCl}_3$ ):  $\delta$  8.07 (s, 1H), 7.73 (t,  $J$  = 6.0 Hz, 1H), 6.27 (s, 1H), 4.39 (br s, 2H), 3.87 (s, 3H), 3.29 (m, 2H), 2.90 (m, 2H), 2.13 (d,  $J$  = 7.0 Hz, 2H), 1.90 (m, 2H), 1.66 (m, 8H), 1.48 (m, 1H), 1.36 (m, 2H), 1.16 (m, 3H), 0.84 (m, 2H);  $^{13}\text{C}$  NMR (100 MHz,  $\text{CDCl}_3$ ):  $\delta$  164.6, 157.4, 146.6, 133.1, 112.0, 111.6, 97.9, 65.9, 56.2, 54.0 (2C), 45.1, 36.0, 35.1, 32.0 (2C), 29.7, 26.7 (2C), 26.1 (2C); LC-MS:  $[\text{M} + \text{H}]^+ = 394.59 - 396.58$ ; IR (KBr):  $\nu$   $\text{cm}^{-1}$  3400, 2925, 2854, 1622, 1593, 1536, 1498, 1256; HRMS ( $m/z$ ) calcd for  $\text{C}_{21}\text{H}_{33}\text{ClN}_3\text{O}_2$   $[\text{M} + \text{H}]^+$  394.225581, found 394.225427.

**tert-Butyl 4-[(4-amino-5-chloro-2-methoxybenzoyl)amino]-methyl]piperidine-1-carboxylate (**20**).<sup>74</sup>** To a solution of 4-amino-5-chloro-2-methoxybenzoic (94 mg, 0.467 mmol) in DMF (3 mL) were added  $\text{Et}_3\text{N}$  (64  $\mu\text{L}$ , 0.467 mmol) and *tert*-butyl 4-(aminomethyl)piperidine-1-carboxylate (100 mg, 0.467 mmol). The mixture was cooled to –5  $^\circ\text{C}$ , and HOBT (63 mg, 0.467 mmol) and EDCI-HCl (90 mg, 0.467 mmol) were then added. The mixture was then stirred for 24 h. After dilution with water, the solution was extracted 3 times with AcOEt. The organic layers were combined, washed 4 times with water, dried over  $\text{MgSO}_4$ , filtered, and concentrated under reduced pressure. The crude residue was purified on silica gel (gradient of elution: DCM to DCM/AcOEt 7/3) to provide 155 mg of desired product. White powder (85%): mp 106–108  $^\circ\text{C}$ ;  $^1\text{H}$  NMR (400 MHz,  $\text{CDCl}_3$ ):  $\delta$  8.08 (s, 1H), 7.77 (t,  $J$  = 5.9 Hz, NH), 6.27 (s, 1H), 4.37 (br s, 2H), 4.09 (m, 2H), 3.72 (s, 3H), 3.30 (m, 2H), 2.66 (m, 2H), 1.70 (m, 3H), 1.42 (s, 9H), 1.16 (m, 2H);  $^{13}\text{C}$  NMR (100 MHz,  $\text{CDCl}_3$ ):  $\delta$  164.7, 157.4, 154.9, 146.8, 133.1, 112.4, 111.6, 97.8, 79.4, 56.2, 45.0, 43.9 (2C), 36.5, 29.9 (2C), 28.5 (3C); LC-MS:  $[\text{M} + \text{H}]^+ = 398.53 - 400.52$ ; IR (KBr):  $\nu$   $\text{cm}^{-1}$  3405, 3339, 2976, 2928, 2852, 1680, 1630, 1595, 1542, 1501, 1425, 1315, 1252, 1173, 1144.

**[1-(Cyclohexylmethyl)-4-piperidyl]methyl 4-amino-5-chloro-2-methoxybenzoate (21).** To a suspension of 4-amino-5-chloro-2-methoxybenzoic acid (101 mg, 0.5 mmol) in dry THF (3 mL) was added CDI (89 mg, 0.55 mmol). The mixture was stirred at rt for 24 h, and then a solution of (1-(cyclohexylmethyl)piperidin-4-yl)methanol (106 mg, 0.50 mmol) in dry THF (2 mL) and NaH 60% (21 mg, 0.55 mmol) were added. This new mixture was stirred 3 days at rt and then

concentrated under reduced pressure. The residue was dissolved in AcOEt, washed with water, dried over  $\text{MgSO}_4$ , and concentrated under *vacuo*. The crude product was then purified on silica gel (gradient of elution: DCM (100%) to AcOEt (100%)). White powder (31%): mp 128–130  $^\circ\text{C}$ ;  $^1\text{H}$  NMR (400 MHz,  $\text{CDCl}_3$ ):  $\delta$  7.81 (s, 1H), 6.29 (s, 1H), 4.45 (br s, 2H), 4.08 (d,  $J$  = 6.0 Hz, 2H), 3.84 (s, 3H), 2.88 (m, 2H), 2.10 (d,  $J$  = 7.1 Hz, 2H), 1.86 (m, 2H), 1.69 (m, 7H), 1.48 (m, 1H), 1.39 (m, 2H), 1.19 (m, 4H), 0.86 (m, 2H);  $^{13}\text{C}$  NMR (100 MHz,  $\text{CDCl}_3$ ):  $\delta$  164.6, 160.2, 147.6, 133.2, 110.0, 109.9, 98.2, 68.9, 66.1, 56.0, 53.9 (2C), 35.6, 35.2, 32.0 (2C), 29.1 (2C), 26.8, 26.2 (2C); LC-MS:  $[\text{M} + \text{H}]^+ = 395.59 - 397.56$ ; IR (KBr):  $\nu$   $\text{cm}^{-1}$  3473, 3330, 2920, 2850, 1695, 1621, 1599, 1449, 1234, 1109; HRMS ( $m/z$ ) calcd for  $\text{C}_{21}\text{H}_{32}\text{ClN}_2\text{O}_3$   $[\text{M} + \text{H}]^+$  395.2101, found 395.2109.

**X-ray Crystallography.** Single crystals of donecopride and compound **17** suitable for X-ray crystallographic analysis were obtained by slow evaporation from a mixture of chloroform/acetone and ethanol, respectively. Data for crystal structures analysis were collected at 150 K with a Bruker–Nonius Kappa CCD area detector diffractometer with graphite-monochromatized Mo  $K\alpha$  radiation ( $\lambda$  = 0.71073  $\text{\AA}$ ). The structures were solved using direct methods and refined by full-matrix least-squares analysis on  $F^2$ .

**Crystallographic Data of Donecopride.** Crystal size: 0.38  $\times$  0.25  $\times$  0.09 mm. Formula  $\text{C}_{22}\text{H}_{33}\text{ClN}_2\text{O}_2$ , formula weight 392.95, crystal system triclinic, space group  $P\bar{1}$ ,  $a$  = 10.5505(3)  $\text{\AA}$ ,  $b$  = 10.6906(4)  $\text{\AA}$ ,  $c$  = 19.8075(6)  $\text{\AA}$ ,  $\alpha$  = 83.6320(10) $^\circ$ ,  $\beta$  = 75.3140(10) $^\circ$ ,  $\gamma$  = 88.2010(10) $^\circ$ ,  $V$  = 2147.78(12)  $\text{\AA}^3$ ,  $Z$  = 4, calculated density = 1.215 g/ $\text{cm}^3$ ,  $\mu$  = 0.197  $\text{mm}^{-1}$ ,  $R_{\text{int}}$  = 0.041,  $R[F2 > 2\sigma(F2)]$  = 0.070,  $wR(F2)$  = 0.196.

**Crystallographic Data of Compound 16.** Crystal size: 0.42  $\times$  0.38  $\times$  0.21 mm. Formula  $\text{C}_{22}\text{H}_{34}\text{ClN}_3\text{O}_2$ , formula weight 407.97, crystal system monoclinic, space group  $P2_1/c$ ,  $a$  = 12.0789(5)  $\text{\AA}$ ,  $b$  = 9.9591(5)  $\text{\AA}$ ,  $c$  = 19.5343(7)  $\text{\AA}$ ,  $\beta$  = 104.580(2) $^\circ$ ,  $V$  = 2274.20(17)  $\text{\AA}^3$ ,  $Z$  = 4, calculated density = 1.192 g/ $\text{cm}^3$ ,  $\mu$  = 0.189  $\text{mm}^{-1}$ ,  $R_{\text{int}}$  = 0.026,  $R[F2 > 2\sigma(F2)]$  = 0.040,  $wR(F2)$  = 0.113.

**Program(s) Used to Solve Structures: SHELXS–97.<sup>75</sup>** Program(s) used to refine structures: SHELXL–2014.<sup>76</sup> Software used to prepare material for publication: SHELXL–2014. Crystallographic data have been deposited at the Cambridge Crystallographic Data Centre, CCDC no. 1045006 (donecopride) and CCDC no. 1045005 (**16**). Copies of this information may be obtained free of charge from the Director, CCDC, 12 Union Road, Cambridge, CB2 1EZ, UK (+44-1223-336408; E-mail: deposit@ccdc.cam.ac.uk or <http://www.ccdc.cam.ac.uk>).

**In Vitro Biological Studies. Pharmacological Characterization of Drugs on Guinea Pig 5-HT<sub>4</sub>R.** Binding to native 5-HT<sub>4</sub>R from guinea pig was determined using the method of Grossman.<sup>61</sup> For membrane preparations male guinea pigs (300–350 g, Charles River) were subjected to euthanasia by cervical dislocation and decapitated. Brains were rapidly removed at 4  $^\circ\text{C}$ , and striatal regions carefully dissected and pooled. The tissues were then suspended in 10 volumes of HEPES buffer 50 mM pH 7.4 at 4  $^\circ\text{C}$ . After homogenization at 4  $^\circ\text{C}$  (Ultra-Turrax, maximal speed, 15 s) and ultracentrifugation (23,000g, 60 min, 4  $^\circ\text{C}$ ), the pellet was resuspended in 10 volumes of HEPES buffer 50 mM pH 7.4 at 4  $^\circ\text{C}$  in order to obtain a tissue concentration of about 100 mg protein/mL. The protein concentration was determined by the method of Lowry<sup>77</sup> using bovine serum albumin as standard.

For radioligand binding studies, 600  $\mu\text{g}$  of membrane was incubated in duplicate at 37  $^\circ\text{C}$  for 30 min with **22** (PerkinElmer), fixed concentration of compound, and HEPES buffer 50 mM pH 7.4 at 37  $^\circ\text{C}$ . Incubation was terminated by rapid vacuum filtration through 0.5% polyethylenimine-presoaked Whatman GF/B filters (Alpha Biotech) using a Brandel Cell Harvester. Filters were subsequently washed three times with 4 mL of HEPES buffer 50 mM pH 7.4 at 4  $^\circ\text{C}$ .

The method was validated from saturation studies: 6 concentrations of **22** were used to give final concentrations of 0.02–0.8 nM; nonspecific binding of **22** was defined in the presence of 30  $\mu\text{M}$  serotonin to determine the  $K_d$  and the Bmax.

For competition studies, **22** was used to give a final concentration of 0.1 nM. Percentages of inhibition of the binding of **22** were obtained for concentrations of 10<sup>-6</sup> and 10<sup>-8</sup> M of the ligands tested. For some of these compounds, affinity constants were calculated from 5-point inhibition curves using the EBDA-Ligand software and expressed as  $K_i \pm \text{SD}$ .

**Pharmacological Characterization of Drugs on Human 5-HT<sub>4</sub>R.** The method was validated from saturation studies: six concentrations of **22** were used to give final concentrations of 0.0625–2 nM, and nonspecific binding of **22** was defined in the presence of 30  $\mu\text{M}$  serotonin to determine the  $K_d$  and the Bmax. For competition studies, 2.5  $\mu\text{g}$  of proteins (5-HT<sub>4B</sub> membrane preparations, HTS110M, Millipore. Millipore's 5-HT<sub>4B</sub> membrane preparations are crude membrane preparations made from their proprietary stable recombinant cell lines to ensure high level of GPCR surface expression) were incubated in duplicate at 25 °C for 60 min in the absence or the presence of 10<sup>-6</sup> or 10<sup>-8</sup> M of each drug and 0.2 nM **22** (VT 240, ViTrax) in 25 mM Tris buffer (pH 7.4, 25 °C). At the end of the incubation, homogenates were filtered through Whatman GF/C filters (Alpha Biotech) presoaked with 0.5% polyethylenimine using a Brandel cell harvester. Filters were subsequently washed three times with 4 mL of ice-cold 25 mM Tris buffer (pH 7.4, 4 °C). Nonspecific binding was evaluated in parallel in the presence of 30  $\mu\text{M}$  serotonin.

For some of these compounds, affinity constants were calculated from 5-point inhibition curves using the EBDA-Ligand software and expressed as  $K_i \pm \text{SD}$ .

**Determination of cAMP Production.** COS-7 cells were grown in Dulbecco's modified Eagle medium (DMEM) supplemented with 10% dialyzed fetal calf serum (dFCS) and antibiotics. Cells were transiently transfected with plasmid encoding HA-tagged 5-HT<sub>4</sub>R, then seeded in 24-well plates (70,000 cells/well). Twenty-four hrs after transfection, cells were exposed to the indicated concentrations of 5-HT<sub>4</sub>R ligands in the presence of 0.1 mM L-ascorbic acid and 0.1 mM of the phosphodiesterase inhibitor RO-20–1724, at 37 °C in 250  $\mu\text{L}$  of HBS (20 mM HEPES; 150 mM NaCl; 4.2 mM KCl; 0.9 mM CaCl<sub>2</sub>; 0.5 mM MgCl<sub>2</sub>; 0.1% glucose; 0.1% BSA). After 10 min, cells were lysed by addition of the same volume of Triton-X100 (0.1%). Quantification of cAMP production was performed by HTRF by using the cAMP Dynamic kit (Cisbio Bioassays) according to the manufacturer's instructions.

**In Vitro Tests of AChE and BuChE Biological Activity.** Inhibitory capacity of compounds on AChE biological activity was evaluated through the use of the spectrometric method of Ellman.<sup>78</sup> Acetyl- or butyrylthiocholine iodide and 5,5-dithiobis(2-nitrobenzoic) acid (DTNB) were purchased from Sigma-Aldrich. Lyophilized BuChE from equine serum (Sigma-Aldrich) was dissolved in 0.2 M phosphate buffer pH 7.4 such as to have enzyme solutions stock with 2.5 units/mL enzyme activity. AChE from human erythrocytes (buffered aqueous solution, ≥500 units/mg protein (BCA), Sigma-Aldrich) was diluted in 20 mM HEPES buffer pH 8, 0.1% Triton X-100 such as to have enzyme solution with 0.25 unit/mL enzyme activity. In the procedure, 100  $\mu\text{L}$  of 0.3 mM DTNB dissolved in phosphate buffer pH 7.4 were added into the 96-well plate followed by 50  $\mu\text{L}$  of test compound solution and 50  $\mu\text{L}$  of enzyme (0.05 U final). After 5 min of preincubation at 25 °C, the reaction was then initiated by the injection of 50  $\mu\text{L}$  of 10 mM acetyl- or butyrylthiocholine iodide solution. The hydrolysis of acetyl- or butyrylthiocholine was monitored by the formation of yellow 5-thio-2-nitrobenzoate anion as the result of the reaction of DTNB with thiocholine, released by the enzymatic hydrolysis of acetyl- or butyrylthiocholine, at a wavelength of 412 nm using a 96-well microplate plate reader (TECAN Infinite M200, Lyon, France). Test compounds were dissolved in analytical grade DMSO. Donepezil was used as a reference standard. The rate of absorbance increase at 412 nm was followed every minute for 10 min. Assays were performed with a blank containing all components except acetyl- or butyrylthiocholine, in order to account for nonenzymatic reaction. The reaction slopes were compared and the percent inhibition due to the presence of test compounds was calculated by the following expression: 100 – ( $v_i/v_0 \times 100$ ), where  $v_i$  is the rate calculated in the presence of inhibitor and  $v_0$  is the enzyme activity.

First screening of AChE and BuChE activity was carried out at a 10<sup>-6</sup> or 10<sup>-5</sup> M concentration of compounds under study. For the compounds with significant inhibition (≥50%), IC<sub>50</sub> values were determined graphically by plotting the % inhibition versus the logarithm of six inhibitor concentrations in the assay solution using the Origin software.

**Propidium Competition Assay.** Propidium exhibits an increase in fluorescence on binding to AChE PAS, making it a useful probe for competitive ligand binding to the enzyme.<sup>79</sup> Fluorescence was measured in a Tecan Infinite M200 plate reader. Measurements were carried out in 200  $\mu\text{L}$  final in 96-well plates. Five U (ee)AChE in 1 mM Tris/HCl, pH 8.0 buffer was incubated for 6 h at 25 °C, with a 150  $\mu\text{L}$  10<sup>-5</sup> M solution of tested compounds. One micromolar propidium iodide 50  $\mu\text{L}$  solution was added 10 min before fluorescence measurement. The excitation wavelength was 535 nm, and that of emission, 595 nm. Each assay was repeated two different times.

**Docking Studies.** For each docked compound a preliminary calculation on its protonation state at pH 7.4 was carried out using standard tools of the ChemAxon Package (<http://www.chemaxon.com/>), and the majority microspecies protonated on one or two nitrogen atoms at this pH was used for docking studies.

The homology model of the (h)5-HT<sub>4</sub>R was built using the high-resolution (2.4 Å) crystal structure of the (h) $\beta$ 2 adrenergic receptor-T4 lysozyme fusion protein bound to carazolol (PDB: 2RH1) under the procedure described.<sup>63</sup>

The crystallographic coordinates of (h)AChE used for docking studies were obtained from X-ray structure of the DPZ/AChE complex (PDB ID 4EY7, a structure refined to 2.35 Å with an R factor of 17.7%).<sup>80</sup>

The docking of donecpride into the (h)5-HT<sub>4</sub>R was carried out with the GOLD program (v5.0) using the default parameters.<sup>81,82</sup> This program applies a genetic algorithm to explore conformational spaces and ligand binding modes. To evaluate the proposed ligand positions, the ChemPLP fitness function was applied in these docking studies. The binding site in the 5-HT<sub>4</sub>R model was defined as a 10 Å sphere centered on the aspartic acid residue Asp<sub>100</sub>. Because the mutagenesis studies have shown that the interaction between the positively ionizable amine of ligands and Asp<sub>100</sub> of 5-HT<sub>4</sub>R is crucial for ligand binding, a hydrogen-bond constraint between positively ionizable amine ligand and OD atom of Asp<sub>100</sub> was used during the docking. Furthermore, special attention was paid during the docking procedure to the following amino acids in the binding site, which were kept flexible: Arg<sub>96</sub>, Asp<sub>100</sub>, Thr<sub>104</sub>, Tyr<sub>192</sub>, Ser<sub>197</sub>, and Trp<sub>294</sub>.

Docking of donecpride into (h)AChE was carried out also by means of the GOLD program with the default parameters. To evaluate the proposed ligand poses, the ChemPLP fitness function was applied. The binding site in the AChE model was defined as a 7 Å sphere from the cocrystallized ligand, DPZ and a water molecule interacting with protonated piperidine ring of DPZ was conserved during the docking (residue number 931).

**In Vivo Biological Studies. Animals.** Adult male NMRI mice (3 months old, weighing 35–40 g) from Janvier laboratories (Le Genest-Saint-Isle, France) were used to perform experiments. Mice were housed by 10 in standard polycarbonate cages in standard controlled conditions (22 ± 2 °C, 55 ± 10% humidity) with a reversed 12 h light/dark cycle (light on at 7 pm). Food and water were available ad libitum in the home cage. All experiments were conducted (between 9 am and 3 pm) during the active–dark phase of the cycle and were in agreement with the European Directives and French law on animal experimentation (personal authorization no. 14–17 for M.B. and 14–60 for T.F.).

**CNS Activity and Acute Toxicity Test.** Behavioral and neurological changes induced by graded doses (1, 10, 100 mg/kg) of the tested derivatives were evaluated in mice, in groups of four, by a standardized observation technique at different times (30 min and 3 and 24 h) after IP administration.<sup>83</sup> Major changes of behavioral data (for example, hypo- or hyperactivity, ataxia, tremors, convulsion, etc.) were noted in comparison to the control group. The approximate DL<sub>50</sub> of the compounds were also calculated through the quantification of

mortality after 24 h. Amphetamine (2 mg/kg) and chlorpromazine (10 mg/kg) were used as stimulant and depressive references, respectively.

**Locomotor Activity.** Locomotion of mice was measured using an actimeter (Imetronic) through infrared detection. Eight individual removable polycarbonate cages (21 cm length, 7 cm wide, and 12 cm high), where each mouse was placed, are disposed in the actimeter. Locomotor activity was measured by recording the number of interruption of beams of the red light over a period of 30 min through an attached recording system to the actimeter. Donecoperide was tested at 1, 3, and 10 mg/kg. Amphetamine (2 mg/kg), chlorpromazine (10 mg/kg), and association 2 (0.1 mg/kg)-DPZ (0.3 mg/kg) were used as stimulant, depressive, and pharmacological references, respectively.<sup>84</sup>

**Spatial Working Memory.** Antiamnesiant activity of tested compounds was evaluated by reversal of scopolamine (0.5 mg/kg)-induced deficit on spontaneous alternation behavior in the Y maze test.<sup>85</sup> The Y maze made of gray plastic consisted of three equally spaced arms (21 cm long, 7 cm wide with walls 15 cm high). The mouse was placed at the end of one of the arms and allowed to move freely through the maze during a 5 min session, while the sequence of arm entries was recorded by an observer. An arm entry was scored when all four feet crossed into the arm. An alternation was defined as entries into all three arms on a consecutive occasion. The number of possible alternation is thus the total number of arm entries minus two; the percentage of alternation was calculated as (actual alternation/possible alternation) 100. Donecoperide was tested at 0.1, 0.3, 3, and 10 mg/kg. Different additional groups (DPZ (0.3 mg/kg) and association 2 (0.1 mg/kg) + DPZ (0.3 mg/kg)) were tested as clinical and pharmacological references, respectively.

**Forced Swimming Test.** The FST<sup>86</sup> was carried out in mice individually forced to swim during 6 min in an open cylindrical container (diameter 12 cm, height 20 cm) with a water depth of 13 cm at 23–24 °C.<sup>87</sup> The duration of immobility, after a delay of 2 min, was measured during the last 4 min. Each mouse was judged to be immobile when it ceased struggling and remained floating motionless in the water, making only those movements necessary to keep its head above water. Animals were not pretested. Donecoperide was tested at 0.3 and 3 mg/kg. Imipramine (16 mg/kg) was used as clinical reference.

**Pharmacological Treatments.** 2 and DPZ hydrochloride were purchased from Tocris (Cookson, UK). Amphetamine (+)-α-methylphenethylamine hemisulfate, chlorpromazine hydrochloride, imipramine hydrochloride, and scopolamine hydrobromide were purchased from Sigma (France). All those pharmacological compounds were dissolved in NaCl 0.9% as the vehicle and were administered IP 30 min before tests, except DPZ and scopolamine which were SC administered 20 and 30 min, respectively, before tests.

**Statistical Analysis.** Results were expressed as mean ± SD and were analyzed by one way analysis of variance (ANOVA), with Statview software. In case of significance, a SNK (Student–Newman–Keuls) post hoc test was realized. Additionally, for the spontaneous alternation test, the percentage of alternation was compared to a theoretical 50% value (random alternation) by an univariate *t* test. Differences were considered as statistically significant if the *p* value was strictly under 0.05.

**Cerebrospinal Fluid (CSF) Collection and sAPPα Quantification.** To explore the effect of acute injection of donecoperide on sAPPα release in vivo, two different groups of WT C57BL/6 mice (*n* = 7/group) received one IP injection of vehicle (0.9% w/v NaCl; 0.2% dimethyl sulfoxide in water) or donecoperide (1 mg/kg). 90 min postinjection, mice were anesthetized and mounted onto a stereotaxic instrument. The neck skin was cut, and subcutaneous tissue and muscles separated with the help of microretractors (Fine Science Tools, Heidelberg, Germany). Mice were then laid down so that the head formed an angle of about 135° with the body.<sup>88</sup> A capillary tube (Borosilicate glass, B100-75-10, Sutter Instruments, Novato, California, U.S.A.) was used to punch the dura mater of the cisterna magna. CSF was collected by capillary action and transferred to 0.5 mL microtubes, immediately frozen in dry ice and stored at –80 °C until use. Once thawed, samples were heated at 60 °C for 5 min as

described in literature<sup>89</sup> and analyzed without further freezing–thawing cycles. ELISA kits from IBL International (Hamburg, Germany) for the dosage of sAPPα (mouse/rat sAPPα assay kit, no. 27415) were used according to the manufacturer's instructions. Reactions were read at 620 and 450 nm using an Infinite 2000 luminescence counter. The sAPPα ELISA kits enable the precise and selective quantification of sAPPα versus sAPPβ.

## ASSOCIATED CONTENT

### Supporting Information

Primary binding test for Donecoperide toward a broad range of receptors. ORTEP diagram of 17. This material is available free of charge via the Internet at <http://pubs.acs.org>.

## AUTHOR INFORMATION

### Corresponding Authors

\*E-mail: christophe.rochais@unicaen.fr.

\*E-mail: patrick.dallemagne@unicaen.fr. Tel.: +33-2-31-56-68-13. Fax +33-2-31-56-68-03.

### Author Contributions

The manuscript was written through contributions of all authors. All authors have given approval to the final version of the manuscript.

### Notes

The authors declare no competing financial interest.

## ACKNOWLEDGMENTS

This work was supported by funding from the Conseil Régional de Basse Normandie, France (Dispositif de Soutien aux Projets de Recherche Emergents), French Agence Nationale de la Recherche Projects MALAD ANR-12-JS007-0012-01 and ADAMGUARD ANR-12-BSV4-008-01, and Ligue Européenne Contre la Maladie d'Alzheimer Grant 12721. The authors gratefully acknowledge the CRIHAN (Centre de Ressources Informatiques de Haute Normandie) as well as the European Community (FEDER) for the molecular modelling software. English language editing of this manuscript was provided by Journal Prep.

## ABBREVIATIONS USED

AD, Alzheimer's disease; ACh, acetylcholine; AChE, acetylcholinesterase; AChEI, acetylcholinesterase inhibitor; CAS, catalytic anionic site; DBS, dual-binding site; DPZ, donepezil; MTDL, multitarget-directed ligands; PAS, peripheral anionic site; P-gp, P-glycoprotein

## REFERENCES

- (1) Stelzmann, R. An English translation of Alzheimer's 1907 paper, "Über eine eigenartige erkankung der hirnrinde. *Clinical Anat.* **1995**, *1*, 429–431.
- (2) World Alzheimer Report 2013: the global economic impact of dementia. *Alzheimer's Disease International Home Page*. <http://www.alz.co.uk> (accessed December 12, 2014).
- (3) Mount, C.; Downton, C. Alzheimer disease: progress or profit? *Nat. Med.* **2006**, *12*, 780–784.
- (4) Melnikova, I. Therapies for Alzheimer's disease. *Nat. Rev. Drug Discovery* **2007**, *6*, 341–342.
- (5) Rosini, M.; Simoni, E.; Minarini, A.; Melchiorre, C. Multi-target design strategies in the context of Alzheimer's disease: acetylcholinesterase inhibition and NMDA receptor antagonism as the driving forces. *Neurochem. Res.* **2014**, *39*, 1914–1923.
- (6) Citron, M. Alzheimer's disease: strategies for disease modification. *Nat. Rev. Drug Discovery* **2010**, *9*, 387–398.

- (7) Kola, I.; Landis, J. Can the pharmaceutical industry reduce attrition rates? *Nat. Rev. Drug Discovery* **2004**, *3*, 711–715.
- (8) Prati, F.; Uliassi, E.; Bolognesi, M. L. Two diseases, one approach: multitarget drug discovery in Alzheimer's and neglected tropical diseases. *MedChemComm* **2014**, *5*, 853–861.
- (9) Morphy, R.; Kay, C.; Rankovic, Z. From magic bullets to designed multiple ligands. *Drug Discovery Today* **2004**, *9*, 641–651.
- (10) Morphy, R.; Rankovic, Z. Designed multiple ligands. An emerging drug discovery paradigm. *J. Med. Chem.* **2005**, *48*, 6523–6543.
- (11) Espinoza-Fonseca, L. M. The benefits of the multi-target approach in drug design and discovery. *Bioorg. Med. Chem.* **2006**, *14*, 896–897.
- (12) Morphy, R.; Rankovic, Z. Fragments, network biology and designing multiple ligands. *Drug Discovery Today* **2007**, *12*, 156–160.
- (13) Korcsmáros, T.; Szalay, M. S.; Böde, C.; Kovács, I. A.; Csermely, P. How to design multi-target drugs. *Expert Opin. Drug Discovery* **2007**, *2*, 799–808.
- (14) Bolognesi, M.; Banzi, R. Novel class of quinone-bearing polyamines as multi-target-directed ligands to combat Alzheimer's disease. *J. Med. Chem.* **2007**, *10*, 4882–4897.
- (15) Meunier, B. Hybrid molecules with a dual mode of action: dream or reality? *Acc. Chem. Res.* **2008**, *41*, 69–77.
- (16) Cavalli, A.; Bolognesi, M. Multi-target-directed ligands to combat neurodegenerative diseases. *J. Med. Chem.* **2008**, *51*, 347–372.
- (17) Morphy, R.; Rankovic, Z. Multi-Target Drugs. Strategies and challenges for medicinal chemists. In *The Practice of Medicinal Chemistry*, 3rd ed; Wermuth, C. G., Ed.; Elsevier: Amsterdam, 2008; pp 549–571.
- (18) Morphy, R.; Rankovic, Z. Designing multiple ligands - medicinal chemistry strategies and challenges. *Curr. Pharm. Des.* **2009**, *15*, 587–600.
- (19) Melchiorre, C.; Bolognesi, M. L.; Minarini, A.; Rosini, M.; Tumiatti, V. Polyamines in drug discovery: from the universal template approach to the multitarget-directed ligand design strategy. *J. Med. Chem.* **2010**, *53*, 5906–5914.
- (20) Hopkins, A. L. Why design multi-target drugs? In *Designing Multi-Target Drugs*; Morphy, J. R., Harris, C. J., Eds.; RCS Publishing: London, 2012; pp 394.
- (21) Lu, J. J.; Pan, W.; Hu, Y. J.; Wang, Y. T. Multi-target drugs: The trend of drug research and development. *PLoS One* **2012**, *7*, e40262.
- (22) Morphy, R.; Rankovic, Z. The physicochemical challenges of designing multiple ligands. *J. Med. Chem.* **2006**, *49*, 4961–4970.
- (23) Schmitt, B.; Bernhardt, T.; Moeller, H. J.; Heuser, I.; Frolich, L. Combination therapy in Alzheimer's disease: a review of current evidence. *CNS Drugs* **2004**, *18*, 827–844.
- (24) Bolognesi, M. L.; Minarini, A.; Tumiatti, V.; Melchiorre, C. Progress in acetylcholinesterase inhibitors for Alzheimer's disease. *Expert Opin. Ther. Pat.* **2006**, *16*, 811–823.
- (25) Zhang, H.-Y. One-compound-multiple-targets strategy to combat Alzheimer's disease. *FEBS Lett.* **2005**, *579*, 5260–5264.
- (26) Youdim, M. B. The path from anti Parkinson drug selegiline and rasagiline to multifunctional neuroprotective anti Alzheimer drugs ladostigil and m30. *Curr. Alzheimer Res.* **2006**, *3*, 541–550.
- (27) Van der Schyf, C. J.; Geldenhuys, W. J.; Youdim, M. B. Multifunctional neuroprotective drugs for the treatment of cognitive and movement impairment disorders, including Alzheimer's and Parkinson's diseases. *Drugs Future* **2006**, *31*, 447–460.
- (28) Bajda, M.; Guzior, N.; Ignasik, M.; Malawska, B. Multi-target-directed ligands in Alzheimer's disease treatment. *Curr. Med. Chem.* **2011**, *18*, 4949–4975.
- (29) Carmo Carreiras, M.; Mendes, E.; Jesus Perry, M.; Paula Francisco, A.; Marco-Contelles, J.; Carreiras, M.; Perry, M.; Francisco, A. The multifactorial nature of Alzheimer's disease for developing potential therapeutics. *Curr. Top. Med. Chem.* **2013**, *13*, 1745–1770.
- (30) Geldenhuys, W. J.; Van der Schyf, C. J. Designing drugs with multi-target activity: the next step in the treatment of neurodegenerative disorders. *Expert Opin. Drug Discovery* **2013**, *8*, 115–129.
- (31) León, R.; Garcia, A. G.; Marco-Contelles, J. Recent advances in the multitarget-directed ligands approach for the treatment of Alzheimer's disease. *Med. Res. Rev.* **2013**, *33*, 139–189.
- (32) Mao, F.; Yan, J.; Li, J.; Jia, X.; Miao, H.; Sun, Y.; Huang, L.; Li, X. New multi-target-directed small molecules against Alzheimer's disease: a combination of resveratrol and clioquinol. *Org. Biomol. Chem.* **2014**, *12*, 5936–5944.
- (33) Tumiatti, V.; Minarini, A.; Bolognesi, M. L.; Milelli, A.; Rosini, M.; Melchiorre, C. Tacrine derivatives and Alzheimer's disease. *Curr. Med. Chem.* **2010**, *17*, 1825–1838.
- (34) Agis-Torres, A.; Söllhuber, M.; Fernandez, M.; Sanchez-Montero, J. M. Multi-target-directed ligands and other therapeutic strategies in the search of a real solution for Alzheimer's disease. *Curr. Neuropharmacol.* **2014**, *12*, 2–36.
- (35) Melchiorre, C.; Andrisano, V.; Bolognesi, M. L.; Budriesi, R.; Cavalli, A.; Cavrini, V.; Rosini, M.; Tumiatti, V.; Recanatini, M. Acetylcholinesterase inhibitors based on a polyamine backbone for potential use against Alzheimer's disease. *J. Med. Chem.* **1998**, *41*, 4186–4189.
- (36) Piazza, L.; Rampa, A.; Bisi, A.; Gobbi, S.; Belluti, F.; Cavalli, A. 3-(4-{[Benzyl(methyl)amino]methyl}-phenyl)-6,7-dimethoxy-2H-2-chromenone (AP2238) inhibits both acetylcholinesterase and acetylcholinesterase-induced  $\beta$ -amyloid aggregation: A dual function lead for Alzheimer's disease therapy. *J. Med. Chem.* **2003**, *46*, 2279–2282.
- (37) Bartolini, M.; Bertucci, C.; Carini, V.; Andrisano, V. beta-Amyloid aggregation induced by human acetylcholinesterase: inhibition studies. *Biochem. Pharmacol.* **2003**, *65*, 407–416.
- (38) Bolognesi, M.; Andrisano, V.; Bartolini, M.; Banzi, R.; Melchiorre, C. Propidium-based polyamine ligands as potent inhibitors of acetylcholinesterase and acetylcholinesterase-induced amyloid- $\beta$  aggregation. *J. Med. Chem.* **2005**, *48*, 24–27.
- (39) Huang, W.; Tang, L.; Shi, Y.; Huang, S.; Xu, L.; Sheng, R.; Wu, P.; Li, J.; Zhou, N.; Hu, Y. Searching for the multi-target-directed ligands against Alzheimer's disease: discovery of quinoxaline-based hybrid compounds with AChE, H<sub>3</sub>R and BACE 1 inhibitory activities. *Bioorg. Med. Chem.* **2011**, *19*, 7158–7167.
- (40) Li, Y.; Peng, P.; Tang, L.; Hu, Y.; Hu, Y.; Sheng, R. Design, synthesis and evaluation of rivastigmine and curcumin hybrids as site-activated multitarget-directed ligands for Alzheimer's disease therapy. *Bioorg. Med. Chem.* **2014**, *22*, 4717–4725.
- (41) Rosini, M.; Simoni, E.; Bartolini, M.; Cavalli, A.; Ceccarini, L.; Pascu, N.; McClymont, D. W.; Tarozzi, A.; Bolognesi, M. L.; Minarini, A.; Tumiatti, V.; Andrisano, V.; Mellor, I. R.; Melchiorre, C. Inhibition of acetylcholinesterase,  $\beta$ -amyloid aggregation, and NMDA receptors in Alzheimer's disease: a promising direction for the multi-target-directed ligands gold rush. *J. Med. Chem.* **2008**, *51*, 4381–4384.
- (42) Muñoz-Ruiz, P.; Rubio, L.; García-Palomero, E.; Dorronsoro, I.; del Monte-Millán, M.; Valenzuela, R.; Usán, P.; de Austria, C.; Bartolini, M.; Andrisano, V.; Bidon-Chanal, A.; Orozco, M.; Luque, F. J.; Medina, M.; Martínez, A. Design, synthesis, and biological evaluation of dual binding site acetylcholinesterase inhibitors: new disease-modifying agents for Alzheimer's disease. *J. Med. Chem.* **2005**, *48*, 7223–7233.
- (43) Bolognesi, M. L.; Cavalli, A.; Valgimigli, L.; Bartolini, M.; Rosini, M.; Andrisano, V.; Recanatini, M.; Melchiorre, C. Multi-target-directed drug design strategy: from a dual binding site acetylcholinesterase inhibitor to a trifunctional compounds against Alzheimer's disease. *J. Med. Chem.* **2007**, *50*, 6446–6449.
- (44) Bolognesi, M. L.; Minarini, A.; Rosini, M.; Tumiatti, V.; Melchiorre, C. From dual binding site acetylcholinesterase inhibitors to multi-target-directed ligands (MTDLs): a step forward in the treatment of Alzheimer's disease. *Mini-Rev. Med. Chem.* **2008**, *8*, 960–967.
- (45) Liu, T.; Xia, Z.; Zhang, W.-W.; Xu, J.; Ge, X.-X.; Li, J.; Cui, Y.; Qiu, Z.-B.; Xu, J.; Xie, Q.; Wang, H.; Chen, H.-Z. Bis(9)-(–)-nor-neptazinol as a novel dual-binding AChEI potently ameliorates scopolamine-induced cognitive deficits in mice. *Pharmacol. Biochem. Behav.* **2013**, *104*, 138–143.

- (46) Minarini, A.; Milelli, A.; Tumiatti, V.; Rosini, M.; Simoni, E.; Bolognesi, M. L.; Andrisano, V.; Bartolini, M.; Motori, E.; Angeloni, C.; Hrelia, S. Cystamine-tacrine dimer: a new multi-target-directed ligand as potential therapeutic agent for Alzheimer's disease treatment. *Neuropharmacology* **2012**, *62*, 997–1003.
- (47) Holmquist, L.; Stuchbury, G.; Berbaum, K.; Muscat, S.; Young, S.; Hager, K.; Engel, J.; Münch, G. Lipoic acid as a novel treatment for Alzheimer's disease and related dementias. *Pharmacol. Ther.* **2007**, *113*, 154–164.
- (48) Bolognesi, M. L.; Minarini, A.; Tumiatti, V.; Melchiorre, C. Lipoic acid, a lead structure for multi-target-directed drugs for neurodegeneration. *Mini-Rev. Med. Chem.* **2006**, *6*, 1269–1274.
- (49) Bolognesi, M. L.; Rosini, M.; Andrisano, V.; Bartolini, M.; Minarini, A.; Tumiatti, V.; Melchiorre, C. MTDL design strategy in the context of Alzheimer's disease: from lipocine to memoquin and beyond. *Curr. Pharm. Des.* **2009**, *15*, 601–613.
- (50) Bolognesi, M. L.; Cavalli, A.; Melchiorre, C. Memoquin: A multi-target-directed ligand as an innovative therapeutic opportunity for Alzheimer's disease. *Neurotherapeutics* **2009**, *6*, 152–162.
- (51) Sterling, J.; Herzig, Y.; Goren, T.; Finkelstein, N.; Lerner, D.; Goldenberg, W.; Miskolczi, I.; Molnar, S.; Rantal, F.; Tamas, T.; Toth, G.; Zagyya, A.; Zekany, A.; Lavian, G.; Gross, A.; Friedman, R.; Razin, M.; Huang, W.; Krais, B.; Chorev, M.; Youdim, M. B.; Weinstock, M. Novel dual inhibitors of AChE and MAO derived from hydroxy aminoindan and phenethylamine as potential treatment for Alzheimer's disease. *J. Med. Chem.* **2002**, *45*, 5260–5279.
- (52) Youdim, M. B.; Amit, T.; Bar-Am, O.; Weinreb, O.; Yogeve-Falach, M. Implications of co-morbidity for etiology and treatment of neurodegenerative diseases with multifunctional neuroprotective-neurorescue drugs: ladostigil. *Neurotoxic. Res.* **2006**, *10*, 181–192.
- (53) Bolea, I.; Gella, A.; Unzeta, M. Propargylamine-derived multitarget-directed ligands: fighting Alzheimer's disease with monoamine oxidase inhibitors. *J. Neural Transm.* **2013**, *120*, 893–902.
- (54) Pisani, L.; Catto, M.; Leonetti, F.; Nicolotti, O.; Stefanachi, A.; Campagna, F.; Carotti, A. Targeting monoamine oxidases with multipotent ligands: an emerging strategy in the search of new drugs against neurodegenerative diseases. *Curr. Med. Chem.* **2011**, *18*, 4568–4587.
- (55) Marco-Contelles, J.; León, R.; de Los Ríos, C.; Guglietta, A.; Terencio, J.; López, M. G.; García, A. G.; Villarroya, M. Novel multipotent tacrine-dihydropyridine hybrids with improved acetylcholinesterase inhibitory and neuroprotective activities as potential drugs for the treatment of Alzheimer's disease. *J. Med. Chem.* **2006**, *49*, 7607–7610.
- (56) Bartolini, M.; Pistolozzi, M.; Andrisano, V.; Egea, J.; López, M. G.; Iriepa, I.; Moraleda, I.; Gálvez, E.; Marco-Contelles, J.; Samadi, A. Chemical and pharmacological studies on enantiomerically pure p-methoxytacrypyrines, promising multi-target-directed ligands for the treatment of Alzheimer's disease. *ChemMedChem.* **2011**, *6*, 1990–1997.
- (57) Cavalli, A.; Bolognesi, M. L.; Capsoni, S.; Andrisano, V.; Bartolini, M.; Margotti, E.; Cattaneo, A.; Recanatini, M.; Melchiorre, C. A small molecule targeting the multifactorial nature of Alzheimer's disease. *Angew. Chem., Int. Ed. Engl.* **2007**, *46*, 3689–3692.
- (58) Lecoutey, C.; Hédou, D.; Freret, T.; Giannoni, P.; Gaven, F.; Since, M.; Bouet, V.; Ballandonne, C.; Corvaisier, S.; Malzert Fréon, A.; Mignani, S.; Cresteil, T.; Boulouard, M.; Claeysen, S.; Rochais, C.; Dallemagne, P. Design of donecpride, a dual serotonin subtype 4 receptor agonist/acetylcholinesterase inhibitor with potential interest for Alzheimer's disease treatment. *Proc. Natl. Acad. Sci. U. S. A.* **2014**, *111*, E3825–E3830.
- (59) Eglen, R. M.; Bonhaus, D. W.; Johnson, L. G.; Leung, E.; Clark, R. D. Pharmacological characterization of two novel and potent 5-HT<sub>4</sub> receptor agonists, RS67333 and RS67506, in vitro and in vivo. *Br. J. Pharmacol.* **1995**, *115*, 1387–1392.
- (60) Lecoutey, C.; Rochais, C.; Genest, D.; Butt-Gueulle, S.; Ballandonne, C.; Corvaisier, S.; Dulin, F.; Lepailleur, A.; Sopkova-de Oliveira Santos, J.; Dallemagne, P. Synthesis of dual AChE/S-HT<sub>4</sub> receptor multi-target directed ligands. *MedChemComm* **2012**, *3*, 627–634.
- (61) Grossman, C. J.; Kilpatrick, G. J.; Bunc, K. T. Development of a radioligand binding assay for SHT<sub>4</sub> receptors in guinea pig and rat brain. *Br. J. Pharmacol.* **1993**, *109*, 618–624.
- (62) Cheung, J.; Rudolph, M. J.; Burshteyn, F.; Cassidy, M. S.; Gary, E. N.; Love, J.; Franklin, M. C.; Height, J. J. Structures of human acetylcholinesterase in complex with pharmacologically important ligands. *J. Med. Chem.* **2012**, *55*, 10282–10286.
- (63) Dubost, E.; Dumas, N.; Fossey, C.; Magnelli, R.; Butt-Gueulle, S.; Ballandonne, C.; Caillard, D.; Dulin, F.; Sopkova-de Oliveira Santos, J.; Millet, P.; Charnay, Y.; Rault, S.; Cailly, T.; Fabis, F. Synthesis and structure-affinity relationships of selective high-affinity S-HT<sub>4</sub> receptor antagonists: application to the design of new potential single photon emission computed tomography (SPECT) tracers. *J. Med. Chem.* **2012**, *55*, 9693–9707.
- (64) Cherezov, V.; Rosenbaum, D. M.; Hanson, M. A.; Rasmussen, S. G.; Thian, F. S.; Kobilka, T. S.; Choi, H. J.; Kuhn, P.; Weis, W. I.; Kobilka, B. K.; Stevens, R. C. High-resolution crystal structure of an engineered human beta2-adrenergic G protein-coupled receptor. *Science* **2007**, *318*, 1258–1265.
- (65) Vickery, R. G.; Mai, N.; Kaufman, E.; Beattie, D. T.; Pulido-Rios, T.; O'Keefe, M.; Humphrey, P. P. A.; Smith, J. A. M. A comparison of the pharmacological properties of guinea-pig and human recombinant S-HT<sub>4</sub> receptors. *Br. J. Pharmacol.* **2007**, *150*, 782–791.
- (66) Brodney, M. A.; Johnson, D. E.; Sawant-Basak, A.; Coffman, K. J.; Drummond, E. M.; Hudson, E. L.; Fisher, K. E.; Noguchi, H.; Waizumi, N.; McDowell, L. L.; Papanikolaou, A.; Pettersen, B. A.; Schmidt, A. W.; Tseng, E.; Stutzman-Engwall, K.; Rubitski, D. M.; Vanase-Frawley, M. A.; Grimwood, S. Identification of multiple S-HT<sub>4</sub> partial agonist clinical candidates for the treatment of Alzheimer's disease. *J. Med. Chem.* **2012**, *55*, 9240–9254.
- (67) Bockaert, J.; Claeysen, S.; Compan, V.; Dumuis, A. 5-HT<sub>4</sub> receptors. *Curr. Drug Targets: CNS Neurol. Disord.* **2004**, *3*, 39–51.
- (68) Li, H.; Robertson, A. D.; Jensen, J. H. Very fast empirical prediction and rationalization of protein pKa values. *Proteins: Struct., Funct., Bioinf.* **2005**, *61*, 704–721.
- (69) Vagedes, P.; Rabenstein, B.; Åqvist, J.; Marelius, J.; Knapp, E.-W. The deacylation step of acetylcholinesterase: computer simulation studies. *J. Am. Chem. Soc.* **2000**, *122*, 12254–12262.
- (70) Fragkouli, A.; Papatheodoropoulos, C.; Georgopoulos, S.; Stamatakis, A.; Stylianopoulou, F.; Tsilibary, E. C.; Tzinia, A. K. Enhanced neuronal plasticity and elevated endogenous sAPPα levels in mice over-expressing MMP9. *J. Neurochem.* **2012**, *121*, 239–251.
- (71) Giannoni, P.; Gaven, F.; de Bundel, D.; Baranger, K.; Marchetti-Gauthier, E.; Roman, F. S.; Valjent, E.; Marin, P.; Bockaert, J.; Rivera, S.; Claeysen, S. Early administration of RS 67333, a specific 5-HT<sub>4</sub> receptor agonist, prevents amyloidogenesis and behavioral deficits in the SXFAD mouse model of Alzheimer's disease. *Front. Aging Neurosci.* **2013**, *5*, 96.
- (72) Tesseur, I.; Pimenova, A. A.; Lo, A. C.; Ciesielska, M.; Lichtenthalter, S. F.; De Maeyer, J. H.; Schuurkes, J. A.; D'Hooge, R.; De Strooper, B. Chronic 5-HT<sub>4</sub> receptor activation decreases Aβ production and deposition in hAPP/PS1 mice. *Neurobiol. Aging* **2013**, *34*, 1779–1789.
- (73) Clark, R. D.; Eglen, R.; Jahangir, A.; Miller, A. B. Gardner, J. O. Preparation of 1–4-aminophenyl)-ω-amino-1-alkanones as 5-HT<sub>4</sub> receptor ligands. WO 1994027965 A1, December 8, 1994.
- (74) Kawakita, T.; Kuroita, T.; Murozono, T.; Hakira, H.; Haga, K.; Ito, K.; Sonda, S.; Kawahara, T.; Asano, K. *Benzoiac acid compounds and use thereof as medicaments*. US 5864039 A, January 26, 1999.
- (75) Sheldrick, G. M. A short history of SHELX. *Acta Crystallogr.* **2008**, *A64*, 112–122.
- (76) Sheldrick, G. M. *SHELXL2014*; University of Göttingen: Göttingen, Germany, 2014.
- (77) Lowry, O. H.; Rosebrough, N. J.; Farr, A. L.; Randall, R. J. Protein measurement with the folin phenol reagent. *J. Biol. Chem.* **1951**, *193*, 265–275.

- (78) Ellman, G. L.; Courtney, K. D.; Andres, V., Jr.; Featherstone, R. M. A new and rapid colorimetric determination of acetylcholinesterase activity. *Biochem. Pharmacol.* **1961**, *7*, 91–95.
- (79) Rosenberry, T. L.; Mallender, W. D.; Thomas, P. J.; Szegletes, T. A steric blockade model for inhibition of acetylcholinesterase by peripheral site ligands and substrate. *Chem. Biol. Interact.* **1999**, *119*–*120*, 85–97.
- (80) Cheung, J.; Rudolph, M. J.; Burshteyn, F.; Cassidy, M. S.; Gary, E. N.; Love, J.; Franklin, M. C.; Height, J. Structures of human acetylcholinesterase in complex with pharmacologically important ligands. *J. Med. Chem.* **2012**, *55*, 10282–10286.
- (81) Jones, G.; Willett, P.; Glen, R. C. Molecular recognition of receptor sites using a genetic algorithm with a description of desolvation. *J. Mol. Biol.* **1995**, *245*, 43–53.
- (82) Jones, G.; Willett, P.; Glen, R. C.; Leach, A. R.; Taylor, R. Development and validation of a genetic algorithm for flexible docking. *J. Mol. Biol.* **1997**, *267*, 727–748.
- (83) Morpugo, C. A new design for the screening of CNS-active drugs in mice. *Arzneim.-Forsch./Drug Res.* **1971**, *11*, 1727–1734.
- (84) Freret, T.; Bouet, V.; Quiedeville, A.; Nee, G.; Dallemande, P.; Rochais, C.; Boulouard, M. Synergistic effect of acetylcholinesterase inhibition (donepezil) and 5-HT(4) receptor activation (RS67333) on object recognition in mice. *Behav. Brain. Res.* **2012**, *230*, 304–308.
- (85) Hooper, N.; Fraser, C.; Stone, T. Effect of purines analogues on spontaneous alternation in mice. *Psychopharmacology* **1996**, *123*, 250–257.
- (86) Porsolt, R. D.; Bertin, A.; Jalfre, M. Behavioral despair in mice: a primary screening test for antidepressants. *Arch. Int. Pharmacodyn. Ther.* **1977**, *229*, 327–336.
- (87) Aguilera, B.; Coulbault, L.; Boulouard, M.; Léveillé, F.; Davis, A.; Tóth, G.; Borsodi, A.; Balboni, G.; Salvadori, S.; Jauzac, P.; Allouche, S. *In vitro* and *in vivo* pharmacological profile of UFP-512, a novel selective delta-opioid receptor agonist; correlations between desensitization and tolerance. *Br. J. Pharmacol.* **2007**, *152*, 1312–1324.
- (88) Liu, L.; Duff, K. A technique for serial collection of cerebrospinal fluid from the cisterna magna in mouse. *J. Visualized Exp.* **2008**, *21*, 960 DOI: 10.3791/960.
- (89) Bourdin, J.; Desire, L.; Schweighoffer, F. Methods and tools for the therapy of neurodegenerative pathologies. WO2008009868, May 8, 2008.